Annu. Rev. Fluid Mech. 1992. 24 : 235–79

VORTEX RINGS[1]

Karim Shariff

Computational Fluid Dynamics Branch, NASA Ames Research Center, Moffett Field, California 94035

Anthony Leonard

Graduate Aeronautical Laboratories, California Institute of Technology, Pasadena, California 91125

KEY WORDS: vorticity dynamics, viscous flows, incompressible and inviscid flows, starting vortices, turbulent vortices, vortex sound

1. CONTEXT AND CONTENT

To interest an engineer in vortex rings one might cite the fact that cavitated rings are used for underwater drilling (Chahine & Genoux 1983), have potential use in fighting oil well fires (Akhmetov 1980) and are used in modeling the downburst, a hazard to aircraft (Lundgren et al 1991). With a physicist one could reason that vortex rings (along with helical vortex tubes and kink waves) admit invariant states and therefore are candidates for "elementary excitations" in turbulence, and one could mention that accelerating ions in superfluid helium create quantized vortex rings (Rayfield & Reif 1963). To a natural philosopher one could explain how dolphins blow vortex ring bubbles and swim through them for amusement (Lundgren & Mansour 1991) and how drops falling into a glass of water form vortex rings. While these are all reasons for making one enchanted with vortex rings, the enduring value of studying them lies elsewhere. One need only look at work of the last century, directed towards proving Kelvin's theory of vortex ring atoms, or at work of two decades ago, sometimes interested in whether vortex rings could be employed to launch

[1] The US Government has the right to retain a nonexclusive, royalty-free license in and to any copyright covering this paper.

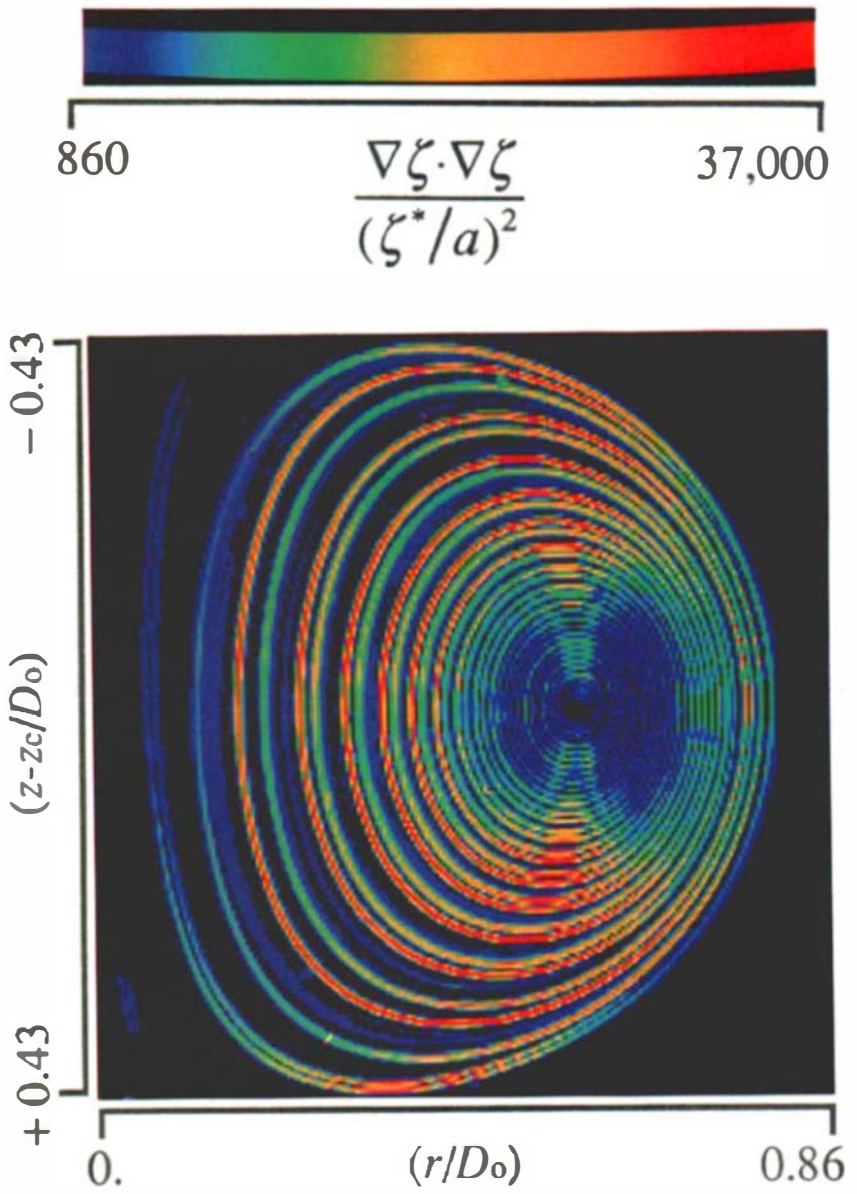

Figure 1 From Southerland et al (1991). Shown is the mixing rate of a tracer in a well-developed laminar vortex ring. The tracer is a dye of Schmidt number ≈ 600 injected into the pipe fluid. The measure of mixing rate depicted is $\nabla c \cdot \nabla c$, where $c(x, \sigma)$ is the concentration field. Notice how the mixing rate diminishes towards the vortex center. This is because adjacent diffused layers have begun to overlap. Contrast this with measurements (Dabiri & Gharib 1991) employing a low Schmidt number tracer (temperature).

pollution wastes to higher altitudes, to see that what survives time are the purely hydrodynamic results concerning the behavior of vorticity and the specific examples that enrich our intuition about vorticity. That the vortex ring has been used to understand various aspects of vortex motion is due to the fact that it is fairly robust, as well as simpler to generate, analyze, and isolate from end-effects than other configurations.

CONTEXT In recent years, vortex rings have been studied in the broader arena of three issues.

1. *Generation of sound.* One probably intuitively appreciates the role vortices play in the generation of sound—according to a linguist (Minahen 1983), "the words 'whirl' and 'whorl,' associated with the vortex, for example the breathy 'wh' in combination with the churning 'rl' indicates something more than simply an arbitrary relationship between the idea and its acoustical image." Möhring (1978) expressed the (quadrupole) sound field directly in terms of vorticity unsteadiness and this led Müller & Obermeier (1988) to take D. Küchemann's (1965) statement that vortices are the "muscles and sinews" of fluid motion and add that vortices might also be called the "voice of the flow." In aeroacoustic experiments it is often difficult to pinpoint individual events as sound sources. Kambe, Minota and their co-workers have been studying the acoustics of mutually interacting rings and rings interacting with edges and bluff bodies (see Minota et al 1988 and references therein). Because their experiments permit identification of the sound source and have often accompanied successful theoretical modeling, theirs has been rightly hailed as one of the few "clean" aeroacoustic experiments.

2. *Transport and mixing.* We also recognize, through our everyday experiences, the role of vortices in mixing. Dimotakis (1984) for instance, describes mixing in shear layers as a two step process: engulfment by the Biot-Savart induced velocity followed by straining of interfaces between species and molecular diffusion. Both steps are exemplified in vortex rings. With respect to the first step, there are two forms of engulfment. One form is that exhibited by any temporally or spatially growing region such as a jet (Taylor 1958). Specifically, a viscous vortex ring carries with it a continually increasing volume of fluid and while this process can be visualized in the limit of self-similar decay (Allen 1984, Cantwell 1986), only a simple model has been constructed for earlier times (Maxworthy 1972, 1974). The mechanism of growth need not be viscous—this form of entrainment is also present in rings expanding due to buoyancy (Turner 1963) and in the growing spiral vortex sheet during ring formation. After formation, the vortex consists of certain fractions of effluent and ambient fluid (Auerbach 1988). The second form of engulfment arises from vorticity fluctuation. It

is illustrated by turbulent vortex rings. Unsteadiness of the vortical core causes ambient fluid to be engulfed into the "atmosphere" of fluid transported with the ring, in exchange for old fluid. This process can be studied for simple models of vortex pairs and rings using dynamical systems theory (Rom-Kedar et al 1990, Shariff et al 1989).

Measurements illustrating the second step of mixing (straining and molecular diffusion) are shown in Figure 1 for the post roll-up phase of a laminar vortex ring. Johari (1990) has performed preliminary experiments of chemical reactions for turbulent rings.

3. *Vortex interactions.* The interaction of vortex tubes is a very complex problem without constraining symmetries. It involves core deformation, vorticity cancellation/merging, change of topology of vortex lines, and intense vorticity stretching. This review discusses axisymmetric (coaxial) interactions and is therefore limited to the first two issues. A vortex near a no-slip wall can create very intense vorticity in the unsteady boundary layer. This vorticity may separate to form other secondary vortices. Production of secondary vorticity reduces the vorticity flux into bluff body wakes and may be the progenitor of "bursting" in the turbulent boundary layer (Robinson 1991).

CONTENT Saffman (1981), in encapsulating the vortex ring problem, said that "one particular motion exemplifies the whole range of problems of vortex motion and is also a commonly known phenomenon, namely, the vortex ring. . . . Their formation is a problem of vortex sheet dynamics, the steady state is a problem of existence, their duration is a problem of stability, and if there are several we have a problem of vortex interactions." We shall do our best to follow this paradigm in organizing this article but sometimes we are forced to a make a division along viscous/inviscid lines. The next section focuses on the problem of formation by discussing how rings are generated naturally and in the laboratory, their resulting structure, and finally, what factors determine whether the rings are laminar or turbulent. Section 3 describes three stages in the life of a laminar ring. Section 4 discusses inviscid dynamics and begins with a discussion of how core dynamics influences overall ring motion (Section 4.1). There are examples of laminar vortices in two dimensions, which attain a balance of nonlinear terms in the inner core; the suggestion that this may be also true of laminar rings is a thread that connects laminar rings to Section 4.2, which discusses the theory of inviscid steady-state rings. Largely however, this body of work stands apart. Unsteady inviscid effects such as mutual straining are discussed in Section 4.3.

In describing how two rings interact along a common axis of symmetry, Section 5 is happily able to unite viscous with inviscid thinking, and

experimental with numerical results. Three types of interactions are considered: "leapfrogging," head-on collisions, and collisions with a no-slip wall. The subject of azimuthal instabilities is taken up in Section 6: The linear instability theory has been reasonably successful in accounting for experimental observation but later stages in the breakdown are not well understood. The last section discusses turbulent vortex rings and puffs.

BASIC NOTATION We employ cylindrical coordinates with axial distance, x, radial distance normal to the symmetry axis, σ, and, azimuthal angle, ϕ. The (Stokes) streamfunction ψ in terms of velocity components is

$$u_x = \frac{1}{\sigma}\frac{\partial \psi}{\partial \sigma}, \qquad u_\sigma = -\frac{1}{\sigma}\frac{\partial \psi}{\partial x}. \tag{1.1}$$

The vorticity will be denoted as $\boldsymbol{\omega}$ and its components as ω with an appropriate subscript indicating direction. For unbounded incompressible flow with velocity decaying algebraically and vorticity decaying exponentially at infinity, the time-integral of forces that generated the flow is the *impulse* $\mathbf{I}$ (Batchelor 1973, Section 7.2):

$$\mathbf{I} = \frac{1}{2}\rho \int \mathbf{x} \times \boldsymbol{\omega}\, d^3x, \tag{1.2}$$

where ρ is the constant fluid density. For the axisymmetric case

$$\mathbf{I} = I\hat{\mathbf{x}} = \rho\pi\hat{\mathbf{x}} \int \omega_\phi(x,\sigma)\sigma^2\, dx\, d\sigma. \tag{1.3}$$

The impulse is related to the linear momentum by

$$\mathbf{I} = \frac{3}{2}\rho \int \mathbf{u}\, d^3x \tag{1.4}$$

and is therefore conserved even in the presence of viscosity in the absence of body forces. The impulse together with the circulation,

$$\Gamma = \int \omega_\phi(x,\sigma)\, dx\, d\sigma, \tag{1.5}$$

leads to a definition for the toroidal radius R_1 of a ring such that

$$I/\rho = \pi\Gamma R_1^2. \tag{1.6}$$

An alternate definition of the radius is the radial vorticity centroid:

$$\bar{\sigma} = \frac{\int \sigma \omega_\phi(x, \sigma)\, dx\, d\sigma}{\Gamma}. \tag{1.7}$$

The characteristic translation speed, axial position, toroidal radius, and core size of the ring will be denoted as U, X, R, and δ, respectively.

2. THE FORMATION PROCESS

In his book, Sommerfeld (1950) concludes an exposition of the classical theory of vortex rings with a note of dissatisfaction: The theory had to be left incomplete with respect to one essential point, the uncertainty about the assumed vorticity distribution in the core. He states that this uncertainty could be removed by investigation of the vortex formation process. Theories make statements about behavior given certain initial idealized characteristics of the vortex while experiments make statements about observations given the parameters of the apparatus such as piston speed and stroke length. An understanding of the formation process can not only serve to bridge the gap between theory and experiment but can lead to better controlled and documented experiments.

Before discussing methods available to determine the characteristics of rings formed at a circular pipe or orifice, which are the most common means of creating rings in the laboratory, we shall in the next subsection canvass some intriguing and less common ways in which vortex rings are generated.

2.1 *Techniques for Producing Vortex Rings*

Of all the techniques for producing vortex rings discussed by M.I.T.'s founder W. B. Rogers (1858), the most intriguing yet the simplest "home-brew" method is to allow a drop of water, lightly colored with milk or food dye, to fall from an eye-dropper or burette into a glass of water. A variation that provides consistency and repeatability is to hold a partially formed drop at the tip of the dropper and slowly lower it until it makes contact with the surface of the water. Surprisingly, a vortex ring is also formed without the drop having any initial kinetic energy, indicating that surface tension is an important source for the energy of the rotational motion (for a half-centimeter drop the surface energy is about four times the potential energy). It is entertaining to toy with different conditions. For example, increasing the concentration of coloring produces a negatively buoyant ring that cascades into many smaller rings (e.g. Chen & Chang 1972).

Thomson & Newall (1885) discovered that as the dropping height was

varied the penetration depth of the ring oscillated; the distance between optimum dropping heights corresponded to the free-fall distance of the drops in one period of vibration, suggesting that a slight ovalness of the drop at impact is somehow important in determining the vortex strength. Indeed, clarifying the view in the earlier work of Chapman & Critchlow (1967), Rodriguez & Mesler (1988) presented photographs of the shape of drops at impact, these show that rings penetrate the pool most when the drop is vertically elongated at impact and vice versa. The paper also shows stunning time-sequence photographs of the generation of the rings in the two cases; the shape of the crater on the pool surface and the deformation of the drop are quite different in the two cases, and this somehow affects the strength or stability of the ring. An explanation of how vorticity of the required sign is generated from torques (e.g. from the baroclinic effect) has not been provided to our knowledge. An element that may or may not be important to the explanation is the collapse of the air-film between the drop and pool fluid. Sigler & Mesler (1990) provide remarkable photographs that show how the thin air-film trapped between the drop and pool fluid forms hundreds of tiny air bubbles, some of which are subsequently entrained into the vortex ring. Oguz & Prosperetti (1989) studied the collapse of the film via a model problem involving two fluid regions connected at a neck. Intuitively one might expect the connecting neck to widen due to surface tension, thus preventing further contact between the liquid masses; this is in effect the picture adopted by Chapman & Critchlow (1967) for the drop impact problem. Contrary to expectation, the model problem illustrated that other points of contact may be established between the fluid masses, trapping the intervening fluid in bubbles.

Another interesting method can be found in the May 1976 issue of *National Geographic* (p. 602). A beautiful photograph shows a diver blowing air rings in water. Initially spherical air bubbles acquire a distribution of surface vorticity due to baroclinic torque. The vorticity causes the spherical volume to deform into a torus after which, experiments (Walters & Davidson 1963) suggest, the circulation remains nearly constant. The rings grow to remarkably large radii as they rise. The growth can be accounted for by the method of Turner (1957) for buoyant rings by noting that the fluid impulse for a slender bubble $I/\rho_{\text{water}} = \pi\Gamma\bar{\sigma}^2[1+\mathcal{O}(\delta/R)]$ must increase at a constant rate due to the buoyancy force. Numerical simulations using a boundary integral method by Lundgren & Mansour (1991) exhibited high frequency oscillations of the radius superimposed on the growth. They provided a momentum balance argument of the type to be discussed in Section 4.1 that yields an appealing interpretation for the growth and, with the incorporation of some $\mathcal{O}(\delta/R)$ effects, gives somewhat similar oscillations.

An attractive alternative scheme for generating vortex rings in the laboratory is to let a shock wave emerge at the open end of a cylindrical shock-tube. One advantage is that vortices approaching the idealized ring may be produced—i.e. they have very large Reynolds numbers and thin cores. Also, as vortex sound is proportional to some power of the propagation velocity, high speed rings produce measurable acoustic signals making possible fundamental studies into the nature of vortex sound. Moreover, shadowgraph and Schlieren visualization techniques, when used to visualize the slightly different density of the core, are not affected by history of the motion as is dye. One type of apparatus is documented in Sturtevant & Kulkarny (1978), Sturtevant (1979), and references therein. The contact discontinuity that forms between the pressurized gas and air can be thought of as a piston that drives fluid between itself and the faster moving shock. Plate 78 in Van Dyke (1982) shows a Schlieren visualization of a ring produced in this way by Sturtevant. A different type of apparatus has been used by Kambe & Minota (1983) to study the acoustic radiation when two vortex rings collide head-on.

2.2 *Models of Ring Formation at a Corner*

The technique most often employed to produce vortex rings is to push fluid through a nozzle with turning angle α (see Figure 2*b*); for $\alpha = 3\pi/2$, one has a cylindrical cavity in a plane wall (Glezer 1988), while for $\alpha = 2\pi$, one has the pipe geometry. The orifice geometry (Figure 2*a*) also has turning angle $\alpha = 2\pi$ and an additional parameter could be defined to distinguish it from a pipe, if desired.

For a given geometry the characteristics of the ring depend on (*a*) history of the piston velocity scaled by the average piston velocity ($\bar{U}_p$) as a function of time normalized by the ejection time (T_e), (*b*) $\mathrm{Re}_p \equiv \bar{U}_p D/\nu$, and (*c*) L/D, where D is the diameter of the exit and $L = \bar{U}_p T_e$ is the piston stroke. For the orifice geometry the ratio of piston to exit diameter is an additional parameter. An equivalent set of parameters can be defined for drivers other than a piston such as a loudspeaker diaphragm. Given the parameters, the problem is to determine the characteristics of the ring produced.

MODEL BASED ON SELF-SIMILAR ROLL-UP So far the only model that attempts to account for vortex sheet evolution during ejection and that gives some insight into the core structure is the model of self-similar roll-up. In order to keep the formation problem free of a time scale, consider piston velocities of the form $U_p(t) = Bt^m$; to evade length scales, consider times during which the size of the spiral δ_s is much larger than the viscous

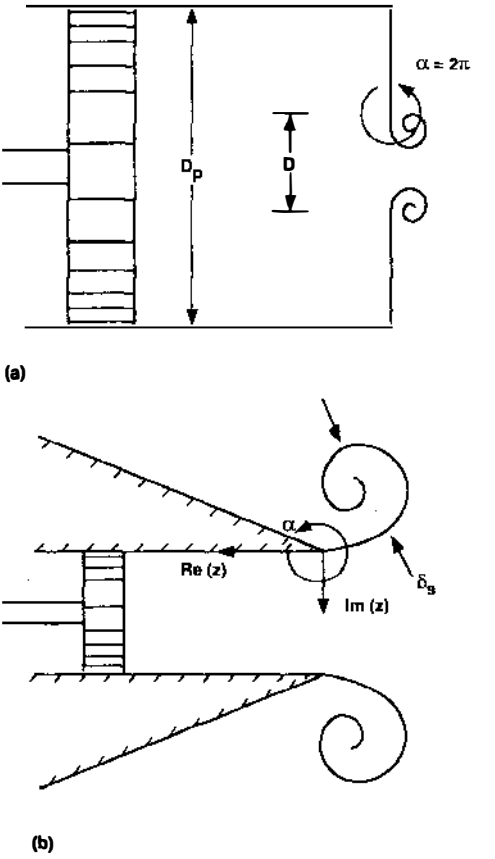

Figure 2 Vortex ring generators. (*a*) orifice geometry, (*b*) nozzle geometry.

scale $(\nu t)^{1/2}$, yet during which there exists a region far away from the spiral where the flow is very nearly turning flow past a two-dimensional infinite wedge. This region lies at distances ϱ from the corner such that $\delta_s \ll \varrho \ll$ distances such as D or D_p at which deviations from the infinite two-dimensional geometry are felt. In this region the flow will be described by the complex potential for two-dimensional flow past a wedge with exterior angle α:

$$\Phi(z) = at^m z^n, \qquad n = \pi/\alpha, \tag{2.1}$$

with z measured as indicated in Figure 2*b*. The constant a can be deter-

mined in terms of B and apparatus geometry by considering the limit in the vicinity of the edge, of the potential flow in the apparatus; for example, Pullin (1979) provides a for a circular hole in an infinite flat plate and for a tube. The only remaining dimensional parameter is a; therefore the spiral must grow in a self-similar fashion with size and circulation

$$\delta_s = C_1(m,n)a^{1/(2-n)}t^{(m+1)/(2-n)}, \qquad \Gamma = C_2(m,n)a^{2/(2-n)}t^{[2(m+1)/(2-n)]-1}. \tag{2.2}$$

C_1 and C_2 are obtained by considering the problem of roll-up of a vortex sheet in turning flow past a two-dimensional wedge (Pullin 1978); the flow is steady in similarity coordinates and the vortex sheet evolution equation becomes an integral equation, which is solved numerically. To obtain the characteristics of rings ejected during a finite duration T_e one may set $t = T_e$ in the above expressions assuming that the ring structure remains frozen for $t > T_e$. In reality, the ring shrinks a little after $t = T_e$ (Didden 1979).

PREDICTION OF STRUCTURE The model of self-similar roll-up together with considerations of the effect of viscosity suggests the form of the vorticity distribution in the core and its dependence on the parameters of the generating process. The vorticity distribution has been deduced by Pullin (1979) and Saffman (1978) based on the work of Moore & Saffman (1973) for aircraft trailing vortices. It is obtained by considering only the innermost windings of the spiral, which are nearly circular. Choosing polar coordinates (ϱ, θ) with origin at the center of the spiral, the radial velocity in the inner region will be negligible and the tangential velocity u_θ will be nearly independent of θ. Hence the amount of sheet material within a circle of radius ϱ must be independent of time as must the circulation $\Gamma(\varrho) = 2\pi\varrho u_\theta$. On the other hand, self-similarity requires

$$\frac{u_\theta(\varrho,t)}{\beta t^{p-1}} = f(\eta), \qquad \eta \equiv \frac{\varrho}{\alpha t^p}, \qquad p \equiv \frac{m+1}{2-n}, \tag{2.3}$$

so that the condition that $\Gamma(\varrho)$ be time independent gives:

$$f(\eta) = C\eta^{(p-1)/p}. \tag{2.4}$$

This line of reasoning is due to Kaden (1931, p. 10). Note that the assumption of radial symmetry has destroyed the discrete structure of the spiral. In the outer region of the spiral (Region I) the distance between spiral turns will be larger than the diffusion thickness and the discrete sheet structure will be present. The velocity distribution (2.4) will hold over an inner region (Region II) in which the diffusion thickness of the sheet exceeds the distance between spiral turns. For an edge ($\alpha = 2\pi$), the velocity

at the center of the spiral is singular if $m < 1/2$. The singularity is resolved by an inner viscous subcore (Region III) of thickness $(\nu t)^{1/2}$. The velocity distribution for this region is obtained solving the tangential momentum equation subject to $u_\theta \sim \varrho^{(p-1)/p}$ as the initial condition and as the boundary condition for $\varrho \to \infty$. The result can be given analytically in terms of a hypergeometric function; the associated vorticity distribution is peaked and decays algebraically.

There is an excellent paradigm here for how a better understanding of the formation process can help merge experiment and theory. Inviscid theories of vortex ring instability (Section 6) predict that the number of waves should depend on a ring speed parameter, given a fixed shape for the vorticity distribution. On the other hand, Leiss and Didden (Saffman 1978) observed that in practice the number of waves changed as this parameter remained constant. Either the theory did not apply to reality or the shape of the vorticity distribution was unexpectedly and drastically altered with varying apparatus parameters. Saffman (1978) took the latter view; he input the hypergeometric velocity distribution into a stability calculation and showed that as the Reynolds number of the apparatus changed, the vorticity distribution in the core changed significantly to account for the experimentally observed change in the number of waves.

SLUG-FLOW MODEL In order to predict the circulation perhaps the best current technique is to use the so-called slug-flow model with some judicious empirical corrections. We make constant reference to Figure 3. The slug-flow model assumes that the velocity external to the boundary layer at the exit plane is the piston velocity so that the flux of vorticity is

$$\frac{d\Gamma_{\text{slug}}}{dt} = \int \omega_\phi u_x \, d\sigma \approx \int -\frac{\partial u_x}{\partial \sigma} u_x \, d\sigma \approx \frac{1}{2} U_p^2(t). \tag{2.5}$$

The integrals extend over the boundary layer; the first approximation sign means boundary layer assumptions are being invoked and the second, that the boundary layer edge velocity is the piston speed. In a sterling piece of work, Didden (1979, 1982) measured the vorticity flux for the pipe geometry and found that the following factors cause the actual flux to be different. 1. The boundary layer edge velocity at the exit is higher than the piston speed due both to the acceleration of the flow around the edge and to the boundary layer displacement effect at later times. This increases the flux through the pipe over the predicted value (see *solid circles* in Figure 3). 2. Ingestion of vorticity of the opposite sign created on the outer pipe wall decreases the circulation (*solid squares*).

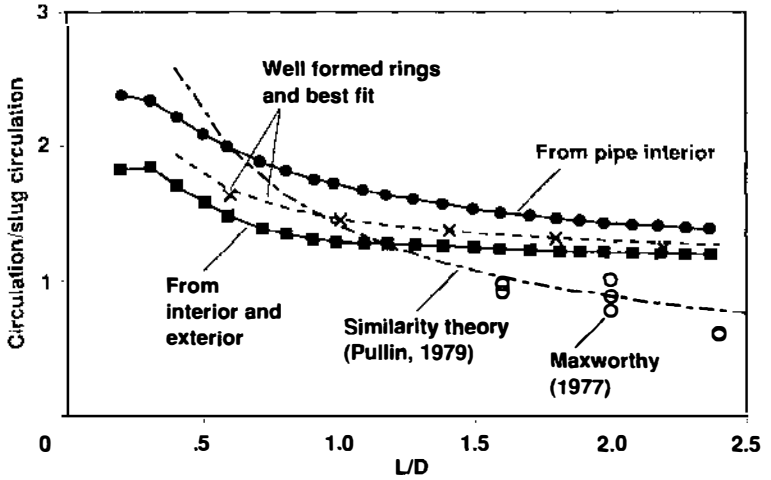

Figure 3 Circulation of vortex rings formed at a pipe referred to the circulation predicted by the slug-flow model, Equation (2.5). Unless indicated, the data are from Didden (1979). The multiple data points of Maxworthy (1977) at the three L/D values are for different Reynolds numbers, increasing downward. Well-formed rings seem to have a larger circulation (*crosses*) than the total flux at the pipe (*solid squares*) due to slight inadequacy in measuring the flux at the pipe.

The experimental data for well-formed rings at some distance from the pipe ($\times$ symbol) is fit well by the dashed line given by

$$\frac{\Gamma}{\Gamma_{slug}} = 1.14 + 0.32(L/D)^{-1}, \qquad L/D > 0.6. \tag{2.6}$$

Didden found that Γ/Γ_{slug} was not very dependent on Re_p in the regime he considered [$\Gamma_{slug}/\nu < 7000$; Figure 4b in Glezer (1988)]. Thus the slug-flow model underpredicts the circulation in this regime and the acceleration effect must dominate. By contrast at higher Reynolds numbers [$\Gamma_{slug}/\nu = 3$–5×10^4; Maxworthy (1977)] the slug-flow model mostly overpredicts the circulation, perhaps indicating greater vorticity cancellation (*open circles*). For the pipe geometry, the model of self-similar roll-up (Pullin 1979) predicts (*chain-dashed curve*)

$$\frac{\Gamma}{\Gamma_{slug}} = 1.41(L/D)^{-2/3}, \tag{2.7}$$

which agrees with Maxworthy's (1977) data but not with Didden's results. The fact that the slug-flow model maintains nearly uniform *absolute* error

with changing L/D and with changing Reynolds number within a certain range has prompted Glezer to suggest the model as a good aid for correlating circulations in a single facility.

EVALUATION OF THE MODEL OF SELF-SIMILAR ROLL-UP Didden (1979) measured the trajectory of the spiral formed at a pipe with uniform piston speed. While the radial motion followed the prediction $\Delta R \sim t^{2/3}$ of the similarity theory, at least up to small piston displacements, the axial motion showed a different power law, $X \sim t^{3/2}$; this is also true for the generation of a planar vortex pair (Auerbach 1987).

To construct better models of the formation process and to design appropriate numerical calculations it is necessary to determine the causes for the failure of the model. An investigation in this direction has been undertaken by Auerbach (1987). He considered several possibilities for the failure. 1. The flow seen by the spiral is not turning flow past a wedge because (*a*) the size of the spiral becomes comparable to the pipe radius or other apparatus length scales (in the course of the investigation, the importance of some length scales was ruled out), or (*b*) the size of the spiral becomes non-negligible compared to the ring radius or to the distance to its pair vortex in 2-D. Since the induced velocity $\sim \Gamma/R$, one expects that this effect by itself should not alter the power law for the behavior of the axial position. 2. The shear layer thickness is comparable to the size of the spiral. Estimates of the thickness of the Stokes layer at the wall for the impulsively started motion indicate that it is important only during the early phase of the roll-up. 3. Secondary vorticity is present.

The stability of the roll-up process is an important issue. Moore (1976) showed that the inner spiral turns of a self-similar roll-up are stabilized against Kelvin-Helmholtz instability by stretching. This seems correct in so far as in Glezer's (1988) experiment, turbulence during roll-up is initiated by Kelvin-Helmholtz instability on the cylindrical slug of fluid behind the main spiral. There is a fairly well defined transition boundary in the $\Gamma_{slug}/\nu, L/D$ plane (Glezer 1988), which determines whether the behavior immediately after the ejection is laminar or turbulent. Another mechanism for initiating turbulence is Rayleigh's centrifugal instability caused by ingestion of secondary vorticity (Maxworthy 1972).

To help study stability and effects listed under (1) above, a numerical study of the roll-up of axisymmetric vortex sheets, using the techniques developed by Krasny (1987) to evolve vortex sheets in two dimensions, would be a worthwhile venture. Either vortex methods that allow production of secondary vorticity or numerical solution of the Navier-Stokes equations would be required for an investigation of secondary vorticity production.

3. LAMINAR VORTEX RINGS

Laminar rings seem to undergo three stages in their development: 1. Relaxation to a "main sequence" state of evolution (Stanaway et al 1988a,b), 2. diffusion of vorticity out to the symmetry axis accompanied by cancellation of vorticity, entrainment of irrotational fluid, and deposition of diffuse vorticity into a trailing wake (Maxworthy 1972), and 3. asymptotic drift (Cantwell & Rott 1988).

3.1 *Relaxation Phase*

For reasons that will become apparent later, we denote as "main sequence behavior," the evolution proceeding from a ring of zero thickness and circulation Γ_0 at $t = 0$. Much is known about the behavior at early times (Saffman 1970). Vorticity will spread in a nearly two-dimensional fashion, namely, as a Gaussian with characteristic core size $\delta = (4\nu t)^{1/2}$, but with correction terms of relative order δ/R. In the vicinity of the core, the velocity will be the same as for a rectilinear vortex with identical vorticity distribution but also with irrotational correction terms of relative order δ/R; forward translation of the ring is the most observable effect of the corrections. Luckily, the speed of forward translation can be evaluated without knowledge of the δ/R corrections to the vorticity provided the speed refers to the motion of the vorticity centroid defined by Helmholtz (1858):

$$\bar{x} = \frac{\int \omega_\phi x \sigma^2 \, dx \, d\sigma}{\int \omega_\phi \sigma^2 \, dx \, d\sigma}. \tag{3.1}$$

Since the denominator is proportional to the impulse, $\bar{x}$ is interpreted as the centroid of impulse elements. The evaluation of speed is made possible by an ingenious relation derived by Helmholtz (Equation 9b with errors) from the inviscid equations of motion,

$$2\frac{I}{\rho}\frac{d\bar{x}}{dt} - 6\pi \int \omega_\phi x \sigma u_\sigma \, dx \, d\sigma = \frac{E}{\rho}, \tag{3.2}$$

which Saffman (1970) shows to be equally valid for viscous flow (E is the kinetic energy). Each term in (3.2) can be evaluated with relative errors of $\mathcal{O}(\delta/R)$ giving the speed as:

$$\frac{d\bar{x}}{dt} = \frac{\Gamma_0}{4\pi\bar{\sigma}_0}\left\{\log\left(\frac{8\bar{\sigma}_0}{\sqrt{4\nu t}}\right) - 0.558 + \mathcal{O}[\delta/R \log(\delta/R)]\right\}. \tag{3.3}$$

Using spectral-method simulations of the Navier-Stokes equations in an unbounded domain, Stanaway et al (1988a,b) studied evolution when cores become thicker. First note that starting from any initial condition the (nondimensional) velocity field $\mathbf{u}\bar{\sigma}_0/\Gamma_0$ at time $t\nu/\bar{\sigma}_0^2$ will depend on the initial vorticity distribution as well as the Reynolds number Γ_0/ν. In the thin core limit of the main sequence, the Reynolds number does not enter as a parameter because nonlinear terms vanish for the two-dimensional circular vortex. However, as rings become fatter, the main sequence evolution becomes segregated in terms of Γ_0/ν. Stanaway et al (1988a,b) found, for initial conditions away from the main sequence, that the behavior of $(\bar{\sigma}_0/\Gamma)d\bar{x}/dt$ collapsed to the main sequence after a transient. How quickly other characteristics of the vortex collapse is unknown but the result suggests that as time progresses the solution becomes universal (with a virtual time origin to be determined) for each Γ_0/ν. With increasing Reynolds number one expects that the relaxation phase will persist longer. However, there are inviscid effects that can also promote equilibration. The most striking example is provided by a perturbed Hill's spherical vortex (Pozrikidis 1986), discussed in Section 4.3.

3.2 *Entrainment and Wake Formation Phase*

To describe entrainment one has to employ the term "vortex ring bubble." It refers to the volume of fluid being instantaneously transported with the ring. This concept is precise only for a steadily translating ring: It is the volume enclosed by the dividing streamline in a reference frame moving with the ring. For an unsteady ring the shape of the dividing streamline depends on which definition of vorticity centroid is adopted. In experiments, the bubble is defined to be the propagating ellipsoidal blob of dye. More precise notions of entrainment are lacking.

As pointed out by Maxworthy (1972), it was Reynolds (1876) who seems to have observed that contrary to Kelvin's inviscid picture the volume of the bubble continually increases due to entrainment of external fluid and its velocity decreases because its momentum has to be shared with a greater mass of fluid. Maxworthy (1972) considered vortex rings with Re based on translation speed and maximum bubble extent of ≈ 600. Flow visualization observations indicated that the speed of the bubble decreased exponentially with distance for a few diameters of travel before decreasing at an even faster rate. This implies that

$$U \sim \frac{1}{t}, \tag{3.4}$$

where time is measured from the virtual origin such that $X(0) = -\infty$. If

the flow is self-similar then all velocity scales evolve as (3.4) and conservation of linear impulse implies that the size of the ring $R^3 \sim t$, a result that fits the data well.

Maxworthy (1972, 1974) provided estimates that account for these relationships and the observed deviations from them. The argument has three ingredients:

1. a mechanism of entrainment to account for growth of bubble volume,
2. the concept of "bubble impulse" together with a hypothesis concerning its loss into a wake,
3. the hypothesis of partial self-similarity, viscous layers being allowed to have their own (viscosity dependent) thicknesses.

With respect to entrainment, irrotational fluid is contaminated with vorticity by diffusion as it flows along the surface of the bubble. Due to an associated loss in total pressure, this fluid is unable to traverse the surface of the bubble and it is entrained into the bubble at a volumetric rate proportional to the speed of propagation and the area of the diffused layer normal to the flow. The thickness of the diffused layer is $\delta_3 = \mathcal{O}(\nu R/U)^{1/2} = \mathcal{O}(\mathrm{Re}^{-1/2}R)$ so that

$$\frac{dR^3}{dt} = \gamma \nu^{1/2} R^{3/2} U^{1/2}. \tag{3.5}$$

Consider next the loss of bubble impulse. The properties of the bubble, for example its speed, will be determined by the vorticity distribution in the bubble. It therefore makes sense to define an impulse-like quantity $I'/\rho \sim \int \omega_\phi \sigma^2 \, dx \, d\sigma$ arising from the bubble only. The flux of this quantity into a wake, via a layer whose thickness is of the same order as δ_3, is

$$\frac{d(UR^3)}{dt} = -\beta \nu^{1/2} R^{3/2} U^{3/2}. \tag{3.6}$$

Equations (3.5) and (3.6) have the solution

$$U = c_1 t^{-1+\varepsilon}, \qquad R = c_2 t^{1/3+\varepsilon/3}, \qquad \varepsilon = -\frac{\beta}{2} \mathrm{Re}_0^{-1/2} \tau_0, \tag{3.7}$$

where Re_0 is the Reynolds number $U_0 R_0/\nu$ at formation and τ_0 is the nondimensional time, $\tau_0 \equiv U_0 t_0/R_0$, elapsed from the virtual origin to the time of formation. Hence at large Reynolds numbers $U \sim t^{-1}$ and $R \sim t^{1/3}$ with small corrections at early times, and large deviations as the amount of bubble impulse lost becomes significant.

Equating the impulse residing in the wake per unit length to the rate of

deposition of impulse per unit translation of the bubble provides the thickness of the wake as $\delta_4 = \mathcal{O}(\mathrm{Re}^{-1/8}R)$, i.e. the wake is very thick.

There are preliminary results from both experiments and computations that give reason to believe that more information about laminar rings will be obtained in the future. With respect to computations, Figure 4 (Stanaway et al 1988a,b) shows the evolution of the vorticity and streamfunction of a ring with an initially Gaussian core and Reynolds number $\Gamma_0/\nu = 500$. The growth of bubble volume and the presence of a thick wake are evident. Near the core center, vorticity contours become more elliptical and nearly parallel to streamfunction contours suggesting a tendency for nonlinear terms to balance [strictly speaking, balance requires $\omega_\phi/\sigma = f(\psi)$]. With respect to experiments, Willert & Gharib (1991) used particle image velocimetry to make preliminary measurements of the time evolving vorticity field of a laminar vortex ring with $\mathrm{Re}_p \approx 1050$. It is hoped that some of the predictions of Maxworthy's theory will be tested and possibly refined in future work. With respect to theory, Maxworthy's model needs to be formalized in the spirit of theories of viscous layers at large Reynolds numbers with a careful matching between the layers. A preliminary attempt at a theoretical study of the diffusion of Hill's spherical vortex was made by Batishchev & Srubshchik (1971).

3.3 *Asymptotic Drift Phase*

Phillips (1956) showed that any unbounded flow that has net linear momentum eventually decays to a unique vortex ring solution of the Stokes equations. As the vortex Reynolds number decreases, the Stokes equations will be a good approximation subsequent to some instant $t = t_0$, say. As $(t - t_0) \to \infty$, only the least decaying modes near wavenumber $\mathbf{k} = 0$ will survive. In physical space, they describe a self-similar vortex ring (with impulse as parameter) for which translational motion has ceased, velocities decay as $[\nu(t-t_0)]^{-3/2}$, and lengths increase as $[\nu(t-t_0)]^{1/2}$. Entrainment of fluid by the Stokes ring is visualized as a sink-type flow in a diagram that depicts particle paths in expanding coordinates, with respect to which the flow becomes steady (Allen 1984, Cantwell 1986).

The Stokes vortex ring does not travel. However, one might expect large time solutions of the Navier-Stokes equations to continue to drift at an ever decreasing speed. How does one obtain this asymptotic drift? We shall first describe a heuristic idea and then a point of view developed in Cantwell & Rott (1988, hereafter CR).

The Stokes ring does have net momentum and fluid particles do drift forward, but due to the absence of nonlinear terms particles do not advect any vorticity. Suppose, however, that one calculated for sport this advection from the full Navier-Stokes equations and expressed the answer in

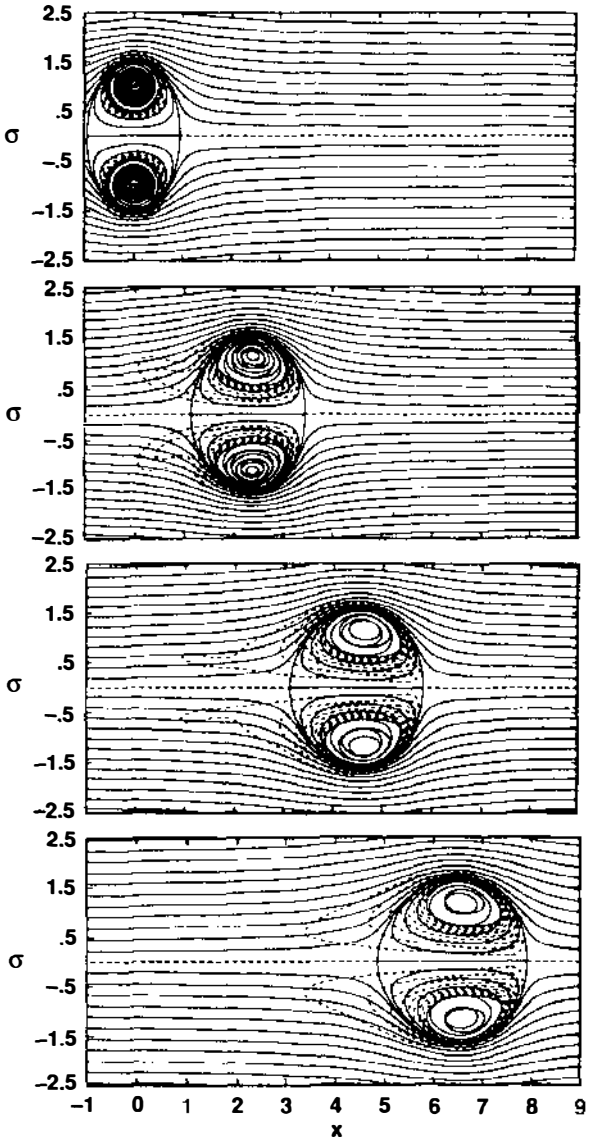

Figure 4 From Stanaway et al (1988a). Calculation of a viscous ring: contours of vorticity and streamfunction relative to a frame moving at the speed of the Helmholtz centroid. To reveal the behavior of weak vorticity, the increment in vorticity between dashed contours was chosen to be 10 times larger than between the solid contours. The initial condition at the top has a Gaussian distribution of vorticity ($\Gamma_0/\nu = 500$).

terms of the motion of Helmholtz's definition of the vorticity centroid. Kambe & Oshima (1975) perform this exercise and find that $d\bar{x}/dt$ has the same power law decay $\sim(t-t_0)^{-3/2}$ as the velocity field of the Stokes solution. CR refer to the result as the asymptotic drift and have given it additional meaning but, before discussing it, some historical remarks are needed.

Kambe & Oshima attempted to obtain the second term in the expansion in terms of inverse powers of time (for the Navier-Stokes equations). In the second-order problem, the Stokes operator acting on the second-order solution is equal to the nonlinear operator acting on the known first-order solution. The second-order solution becomes arbitrarily large compared to the first-order solution at large distances from the origin; a similar nonuniformity occurs for Stokes flow past a sphere (Whitehead's paradox).

CR show that a *uniformly valid* second approximation can be obtained after impressing a spatially uniform drift on the first-order solution. The required drift velocity happens to be the same as that obtained from the procedure of Kambe & Oshima. The result is

$$\frac{d\bar{x}}{dt} = 0.0037038\frac{I/\rho}{[\nu(t-t_\bullet)]^{3/2}}. \tag{3.8}$$

Numerical simulations from a wide variety of initial conditions (Stanaway et al 1988a,b) found exactly the behavior predicted by (3.8) in the final stages of decay. Hence, the asymptotic drift does have meaning for the decay of a vortex ring proceeding from the Navier-Stokes equations. The second-order solution of CR contains an undetermined constant, which reflects loss of information about the nonlinear part of the evolution.

4. INVISCID DYNAMICS

4.1 *Speed of Propagation of Thin Vortex Rings*

An important problem in the dynamics of vortices and in the development of vortex methods (Leonard 1985) is the determination of the "overall" motion of a vortex tube given its core structure. By "overall" motion we mean the evolution of a small number of degrees of freedom, for example, a suitably chosen space curve and core structure parameters along the curve.

We have already discussed Helmholtz's method for computing the translation speed of thin rings without knowing $\mathcal{O}(\delta/R)$ corrections to the vorticity. This is the technique that Kelvin most likely used to obtain the speed for a thin steady ring with ω_ϕ/σ = constant (Lamb 1932, Section 163), the locally two-dimensional solution being a circular core with uni-

form vorticity. Using the same technique, Moore (1980) showed that if the core is elliptical, it rotates at the constant angular velocity of the two-dimensional Kirchhoff elliptic vortex and the propagation speed fluctuates in time.

A way of obtaining the speed that is more physically appealing and applicable to three-dimensional tubes is to balance momentum for a vortex tube section. The method has been used by Widnall & Bliss (1971) and Moore & Saffman (1972) for three-dimensional vortex tubes and by Moore (1985) in which he obtains a compressibility correction to Kelvin's formula. The nice thing is that, as in the Helmholtz method, one does not need to know how the streamlines are distorted from the rectilinear vortex. The following force terms are important at leading order in curvature:

1. a Kutta lift acting in the radial direction away from the symmetry axis, proportional to the speed of the ring;
2. several forces arising from tube curvature; their net effect opposes lift: (*a*) the so-called vortex line tension, which acts towards the center of curvature and results from the pressure difference created by increased velocity on the concave side due to contraction of area, (*b*) a force arising from low pressure on the curved wall of the tube due to the rotating flow that reduces effective tension, and (*c*) an increase in effective tension via suction pressure forces on the end faces of the tube, due to the rotating flow.

Balance of (1) and (2) gives the speed of the ring. Many terms that appear to be missing from this list, for example, the product of virtual mass and acceleration are of higher order in curvature.

The force balance approach allows one to quickly deduce the consequences of many interesting effects. (*a*) A buoyant vortex ring will grow in radius because a Kutta lift needs to be generated in the axial direction to oppose buoyancy (Lundgren & Mansour 1991). A similar effect occurs for ion-tagged superfluid vortex rings subjected to an electric field (Rayfield & Reif 1964). (*b*) A cavitated vortex ring with surface tension will move faster than one without because greater Kutta lift is required to balance the net effect of surface tension force and excess pressure inside the bubble (Moore & Saffman 1972, Chahine & Genoux 1983). (*c*) Swirl (a velocity in the azimuthal direction) slows the ring because centrifugal force helps lift (Widnall & Bliss 1971).

4.2 *Steadily Translating Inviscid Vortex Rings*

Planar calculations of the Navier-Stokes equations depict the emergence of vortex pairs and isolated vortices that have steady inviscid structure in which nonlinear terms have balanced over a large portion of their cores

(Couder & Basdevant 1986, McWilliams 1984). The balance is achieved when the vorticity is some arbitrary function of the streamfunction, i.e. $\omega_z = g(\Psi)$ in 2-D and $\omega_\phi/\sigma = f(\psi)$ for axisymmetric flow. It has been suggested that the principle that chooses $g(\Psi)$ is selective decay of enstrophy by viscosity with energy remaining almost constant (Leith 1984). At present it is difficult to state the degree to which balance is achieved for laminar rings, for instance in the experiments of Sullivan et al (1973) who depict $f(\psi)$ from a limited set of LDV measurements and in the computations of Stanaway et al (1988a).

This possibility, together with the fact that steady vortex rings can be used as initial conditions for studies of interactions and stability, motivate this section.

PROBLEM STATEMENT For inviscid swirl-free axisymmetric flow the equation for the azimuthal vorticity is (Batchelor 1973, p. 508)

$$\frac{D(\omega_\phi/\sigma)}{Dt} = 0. \tag{4.1}$$

The equation describes the convection of vortex lines and the purely geometric stretching of the vorticity. We consider flows that are steady in a reference frame translating with the vortex. The speed of the frame is determined as part of the solution. The condition for steadiness is that ω_ϕ/σ be constant on streamlines, that is $\omega_\phi/\sigma = f(\psi)$, where $f(\psi)$ is an arbitrary function. Then the streamfunction-vorticity relation

$$D^2\psi = \frac{\partial^2\psi}{\partial x^2} + \frac{\partial^2\psi}{\partial\sigma^2} - \frac{1}{\sigma}\frac{\partial\psi}{\partial\sigma} - \sigma^2 f(\psi), \tag{4.2}$$

together with the condition of uniform flow at infinity defines the elliptic problem to be solved. Note that the operator D^2 is not the Laplacian due to the sign of the last term. One is usually interested in solutions for which the vorticity vanishes at infinity. The known axisymmetric solutions are exclusively those in which the vorticity is confined, i.e. where $f(\psi)$ vanishes outside some region $\mathscr{D}$. One then has to solve (4.2) separately in the interior and exterior of $\mathscr{D}$ subject to the conditions of constant ψ and continuous tangential velocity on the boundary of $\mathscr{D}$. The latter condition has been omitted sometimes, resulting in a vortex sheet on the boundary (O'Brien 1961, Durst & Schonung 1982). The problem outlined above is difficult because the shape of the boundary is unknown.

THE CASE $f(\psi)$ = CONSTANT We now discuss the case, popular for over a century, in which $f(\psi)$ = constant in $\mathscr{D}$ and zero everywhere else. This is also the case referred to in the Prandtl-Batchelor theorem (Batchelor 1956)

for the form of a steady recirculating eddy behind axisymmetric bodies at vanishingly small but nonzero viscosity. For example, in computing steady flow past a sphere, Fornberg (1988) found that the recirculating eddy at sufficiently large Reynolds number has $f(\psi)$ very nearly constant and resembles Hill's spherical vortex.

In the limit of thin cores the vorticity becomes uniform and we have already discussed Kelvin's solution for this case. Dyson (1893) considered thicker cores and in a paper that Fraenkel (1972) called "bewildering to modern eyes," investigated, among many other things, corrections to the circular shape up to fourth order in δ/R. At $\mathcal{O}(\delta/R)$, streamlines remain circular but become nonconcentric (Fraenkel 1972, Fetter 1974). The shape starts to become elongated in the axial direction at $\mathcal{O}(\delta^2/R^2)$ due to the strain induced by the curvature of the ring. At the opposite limit, Hill (1894) discovered that a spherical core was also steady. In this case, (4.2) is amenable to solution by separation of variables. These solutions led Batchelor (1967, p. 526) to expect that a continuous family of steady rings ranging from a ring of zero cross-section to Hill's vortex may exist and indeed, Norbury (1973) exhibited specific solutions in the entire range. Norbury's method consisted of writing down the formal solution of (4.2) in terms of the Green's function of the D^2 operator. The problem is thus recast as an integral equation, the unknown being the domain of integration. He solved the problem numerically, approximating the integral by plane quadratures. We shall refer to the class of rings with $f(\psi) =$ constant as the Norbury-Fraenkel (NF) family.

EXISTENCE PROOFS FOR GENERAL $f(\psi)$ There is a mathematical literature on proofs of existence of steady vortex rings. It is not our place to discuss the technical details but there are some interesting results of physical importance that deserve mention.

Variational statements used in existence proofs often have interesting physical consequences and they can be used to develop efficient numerical solution techniques (Eydeland & Turkington 1988). For example, Benjamin (1976) posed the following variational form of the problem of steady confined vortex rings: Start with a given vorticity distribution $\tilde{g}(x, \sigma)$ and imagine rearranging it by convecting it about, preserving impulse while doing so; among all the rearrangements, the ones that maximize the kinetic energy are steady solutions. Note that in this formulation one does *not* prescribe a vorticity function $f(\psi)$. Rather, if the variational problem has a solution, to every specified $\tilde{g}(x, \sigma)$ there will correspond a certain $f(\psi)$ that is unknown beforehand. There is an alternate variational formulation due to Fraenkel & Berger (1974), which although more cumbersome has the advantage that $f(\psi)$ is prescribed.

The energy maximization property has an interesting consequence. Since perturbed vortices (within the stated class) have less energy than the steady state, the allowance of slight compressibility and radiation of energy by sound leads to growth of perturbations (Kop'ev & Leont'ev 1988).

A remarkably simple and constructive method for demonstrating the existence of steady rings is due to Moffatt (1986). He exploits the analogy between the steady Euler equations and the equations for magnetostatics in a fluid with infinite magnetic conductivity:

$$\mathbf{j} \times \mathbf{B} = \nabla p, \qquad \mathbf{j} = \nabla \times \mathbf{B}, \qquad \text{(Magnetostatics)}, \tag{4.3a}$$

$$\boldsymbol{\omega} \times \mathbf{u} = -\nabla H, \qquad \boldsymbol{\omega} = \nabla \times \mathbf{u}, \qquad \text{(Euler equations)}, \tag{4.3b}$$

where $\mathbf{j}$ is the current density, $\mathbf{B}$ is the magnetic field intensity, and $H = p/\rho + \frac{1}{2}\mathbf{u}^2$ is the Bernoulli head. The advantage of the analogy is that one is assured, through the continual dissipation of kinetic energy by viscosity, that the magnetohydrodynamic equations will tend to a steady state described by (4.3a). The disadvantage however is that, as in Benjamin's method, one has no control over $f(\psi)$. Rather, the structure of the vortex ring is controlled by the volume $V(\chi)$ of each magnetic flux tube (χ = constant) in the initially chosen axisymmetric magnetic field. As the relaxation to steady state proceeds, $V(\chi)$ remains constant (because magnetic flux tubes are material) and gives the volume distribution $V(\psi)$ for the Euler solution; the relation between $V(\psi)$ and $f(\psi)$ may be quite complicated.

STEADY AXISYMMETRIC RINGS WITH SWIRL Interest in axisymmetric flows with a velocity component, called swirl, around the symmetry axis stems partly from the occurrence of nearly axisymmetric breakdown bubbles in leading edge vortices over delta wings. We shall however limit ourselves here to discussing isolated ring-like solutions in which swirl is confined to the same region as the azimuthal vorticity.

The problem of the existence of steady solutions has been addressed by Turkington (1986) and Moffatt (1988). Specific solutions are known only for a two-parameter family. They are obtained as solutions to the vorticity streamfunction Equation (4.2); the streamfunction now describes the projection of the velocity vector in an azimuthal plane. The analog of the condition $\omega_\phi/\sigma = f(\psi)$ for steadiness changes. First, by Kelvin's theorem the circulation $K = 2\pi\sigma(x, \sigma, t)u_\phi$ of a circular material line wrapped around the symmetry axis, will remain constant following the line. Hence, $K = K(\psi)$. Secondly, the steady momentum equation (4.3b) implies that velocity vectors lie on surfaces of H = constant so that $H = H(\psi)$. Benjamin (1962) uses a vector diagram to express the azimuthal vorticity in terms of the two arbitrary functions H and K as

$$\omega_\phi = \frac{K(\psi)K'(\psi)}{\sigma} - H'(\psi)\sigma, \tag{4.4}$$

which is the condition required for steadiness (primes denote differentiation with respect to the argument). The known solutions are for the case $H(\psi) = H_0 + \hat{\lambda}\psi$ in the core, $H = H_0$ in the exterior potential flow, and $K(\psi) = \pm\hat{\alpha}\psi$ in the core and zero in the exterior swirl-free region.

The swirl-free limit $\hat{\alpha} = 0$ corresponds to the linear vorticity distribution and the NF family—in particular, Hill's vortex—are solutions. As the swirl parameter $\hat{\alpha}$ is increased, it turns out, rather nicely, that the modified Hill's vortices remain spherical. These solutions are given by Moffatt (1969) and they can be obtained via separation of variables. The force balance argument does not apply for such a thick core and the speed of translation of Hill's vortices with small swirl is actually larger than in the swirl-free case. Swirling extensions of toroidal members of the NF family have been obtained by Eydeland & Turkington (1988, and private communication) using a variational approach geared to efficient numerical solution. They found that for all solutions the angular impulse was bounded by a constant times the linear impulse, suggesting that steady solutions arc possible only up to a critical level of swirl. The limit $\hat{\lambda} = 0$ gives flow (called Beltrami) in which the vorticity is parallel to the velocity: $\mathbf{u} = \pm\hat{\alpha}\boldsymbol{\omega}$ and streamlines coincide with vortex lines.

4.3 *Unsteady Behavior*

Contour dynamics methods have provided much insight into the evolution of two-dimensional patches with uniform vorticity [see Pullin (1992) in this volume]. A similar approach is possible for vortex rings. Equation (4.1) shows that if the vorticity $\omega_\phi = A_i\sigma$, in each region $\mathscr{D}_i$ where A_i is a constant for the region, then it remains so for all time. Hence one needs to track only the motion of the boundaries of $\mathscr{D}_i$ as they advect with the local fluid velocity. A number of workers have independently developed expressions for the induced field in terms of contour integrals around the boundaries of $\mathscr{D}_i$ that reduce the problem to one dimension. Poppe (1978, 1980) considered steady flow, derived an expression for the streamfunction, and found steady solutions with nested contours. Pozrikidis (1986) and Shariff ct al (1989) derived expressions for the velocity field and investigated unsteady behavior.

Moffatt & Moore (1978) studied the linear stability of Hill's spherical vortcx to pcrturbations of the boundary. They found that if the vortex is squashed so that initially its long dimension is along the axis of symmetry, it sheds a tail of volume proportional to the disturbance amplitude from its rear stagnation area. From contour dynamics calculations, Pozrikidis

(1986) found that even for very large perturbations the vortex returned to being spherical after shedding vorticity into a tail. If the vortex is squashed the other way, irrotational fluid enters through a spike from the rear creating a torus from a sphere (aside from a thin spherical cap).

Mutual straining is an important inviscid effect that needs to be considered whenever vortex rings interact. Much of the important physics is captured by a simple model, which assumes that the cores remain elliptical. In two dimensions there exists an early model of Saffman (1979), which can be described as quasi-steady and a later unsteady model due to Melander et al (1986), which has been used to develop successful criteria for the merger of vortices (Melander et al 1988). An elliptical core model has also been developed for vortex rings (Shariff et al 1989): It represents the limiting behavior of contour dynamics for thin and widely separated rings. The idea is that the boundary of the vortex consists of a self-induced motion and a motion induced by other vortex rings. The self-induced motion is given by Moore's (1980) elliptic core solution. The motion induced by other rings is taken to be a rigid translation together with a uniform plane strain and an additional strain required to preserve volume. The result is a system of ordinary differential equations for the five degrees of freedom for each vortex: axial position, radius, major axis, minor axis, and angle.

5. COAXIAL INTERACTIONS

5.1 *Passage Interactions*

If two vortex rings have the same sense of rotation, they travel in the same direction and, under certain conditions, the rear vortex will attempt to pass through the front one. One reason for studying such interactions is that they are observed in a round jet under certain conditions and they may play important roles in sound generation and mixing (Crighton 1980, Hussain & Zaman 1980, Zaman 1985).

Vortex ring models of the last century were inviscid and ignored core deformation; for rings of identical circulation they predict periodic leapfrogging (e.g. Dyson 1893): due to mutual induction the leading vortex widens and travels more slowly while the pursuer shrinks, travels faster, and penetrates the first; the process repeats ad infinitum. Following a period of questioning of whether a "clean" passage could be realized in the laboratory (Maxworthy 1972, Oshima et al 1973, compare p. 524f in the 1967 and 1973 editions of Batchelor), photographic proof was finally provided by Yamada & Matsui (1978).

What are the factors then, which lead to a successful passage? Assuming that two identical rings are produced, the space of governing parameters includes the initial shape of the vorticity distribution (which has as one

parameter the ratio of the initial core size to toroidal radius R), the reduced initial separation d/R, and the Reynolds number.

Inviscid core deformation is one factor and the contour dynamics approach and its associated elliptic core model allows one to make statements about the effect of the first two parameters (Shariff et al 1988, 1989). Using the elliptic model, three outcomes of the interaction were observed which, in essential respects, paralleled those predicted by contour dynamics. 1. Continued leapfrogging with weak "quasi-periodic" core deformation was observed for only the thinnest cores. 2. For thicker cores, a resonance type phenomenon took place in which at each passage the aspect ratio of the initially rear vortex was kicked to a successively higher value, with unabated elongation at some nth passage. 3. For even thicker cores there was unabated elongation of the passing vortex at the very first passage. This is analogous to "vortex tearing" for planar flow (Moore & Saffman 1975b) in which an equilibrium vortex in a straining field becomes unstable at a critical value of the strain-rate, however, elongation occurs at lower strain-rates for leapfrogging rings because time-variation of strain is important.

Now consider the passage experiment of Yamada & Matsui (1978) shown in Figure 5. One suggestion is that the results are not of the third outcome even though the visualization might suggest such a classification. Dyson's circular core model (type 1 outcome) was used to compute unstable manifolds associated with particle motions and the results are shown in Figure 5 compared with the visualization of Yamada & Matsui (1978). The agreement of even fine-scale features suggests that the unstable manifold is a type of attractor and furthermore that, in the experiment, only irrotational or weakly vortical fluid is deforming in the manner depicted by smoke, with vortical cores remaining nearly circular.

However, another factor is *viscous diffusion*. Maxworthy (1979) has commented that in the experiment of Yamada & Matsui ($\mathrm{Re_D} \equiv U_0 D/\nu \approx 1600$) there is likely to be greater merging of the vorticity than suggested by smoke. This is illustrated in Figure 6, which shows calculations by Stanaway et al (1988a) using a spectral method. Because $\mathrm{Re_D} \approx 609$ for the simulation there is probably less merging and deformation in the experiment. Parameters are the same as those of the inviscid calculation shown in Figure 5, the core size being defined where the maximum vorticity occurs. The first passage is successful but note that the initially leading vortex has spread more after the passage because of its different strain history, a process which could be understood by coupling the solution of a diffusing line vortex in an axisymmetric strain (Kambe 1984) with Dyson's (1893) model. This vortex is so weakened that it is unable to resist straining during its own passage. The truth about what is actually occurring in the

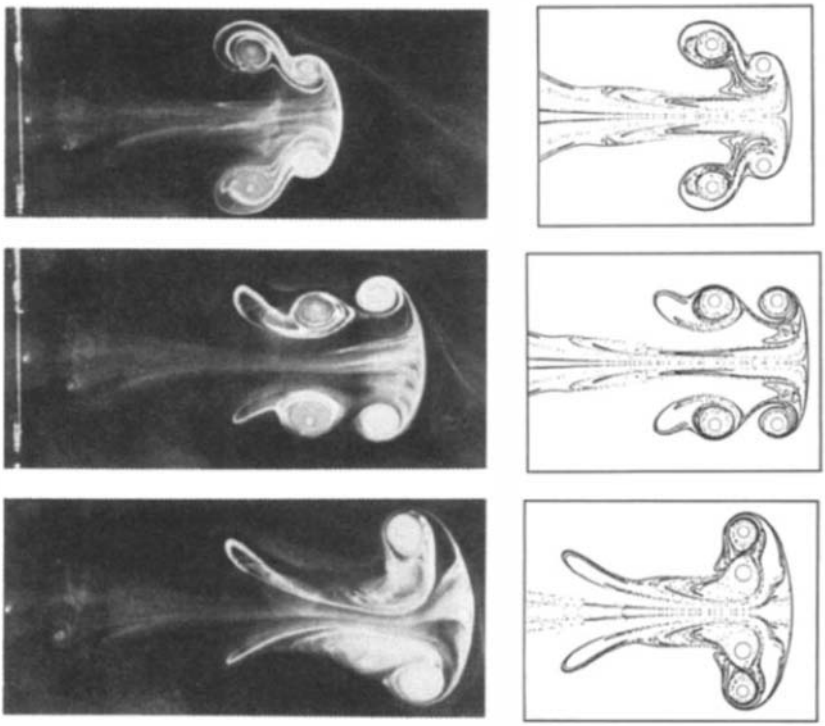

Figure 5 From Shariff et al (1989). Unstable manifold for leapfrogging vortex rings. Photographs are from Yamada & Matsui (1978). The circles in computational figures are the vortex cores, assumed to be in solid body rotation.

experiment is probably a synthesis of the viscous and inviscid results presented. Finally, a third factor that may confront experiments at higher Reynolds numbers is the amplification of azimuthal waves by the mutual straining of the vortices.

Since the passage interaction has some features in common with pairing in a round jet, it is of interest to study the generation and sound using Möhring's (1978) theory. In many instances of passage calculated with contour dynamics, the acoustic power was dominated by a contribution at a frequency equal to half the vorticity, arising from elliptic mode core oscillations. Inspection of the jet-rig noise spectra of Zaman (1985) indicated that peaks closely corresponded to half the maximum phase averaged vorticity for the forced vortex pairing mode as well as the so-called preferred mode, suggesting that a similar mechanism is at work (Shariff et al 1989).

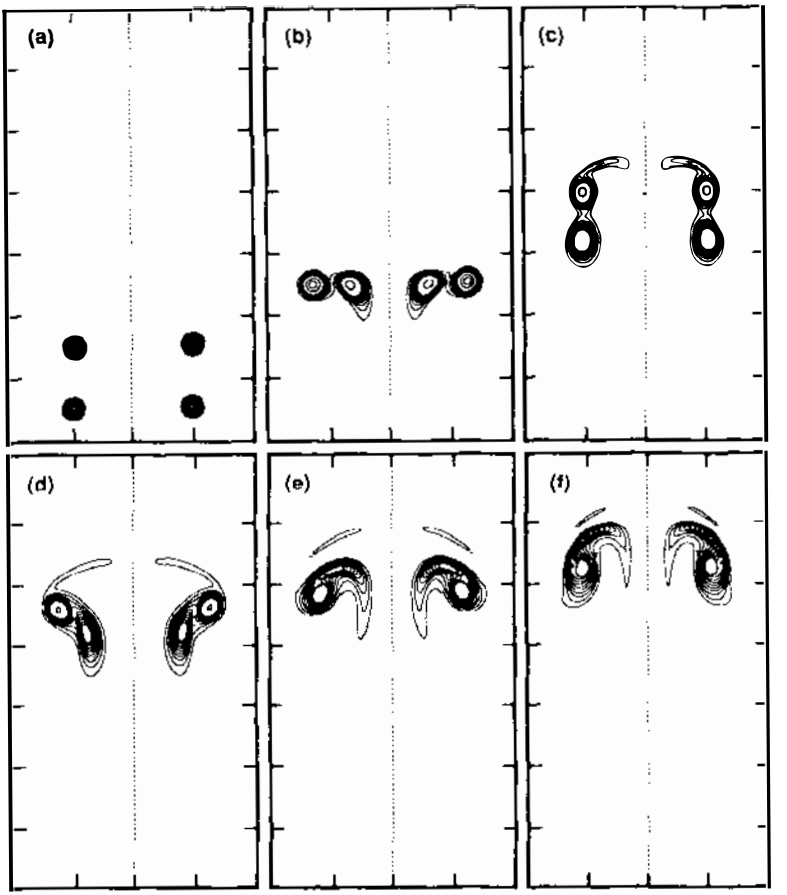

Figure 6 From Stanaway et al (1988a). Vorticity contours for leapfrogging of viscous vortex rings ($\Gamma_0/\nu = 1000$, $Re_D \approx 609$). The computational "mesh" translates with the rings. If the initial peak vorticity is denoted ω_{0p}, level increments are $0.09\omega_{0p}$ between the inner thicker lines and $0.009\omega_{0p}$ between the outer thinner lines. The outermost contour level is $0.01\ \omega_{0p}$.

5.2 *Head-on Collisions*

When two vortices have opposite senses of rotation and are travelling towards each other, their radii grow due to mutual induction and they decelerate. The reasons for studying collisions are indirect. Collisions shed light on what happens when two counter-rotating three-dimensional vortex tubes interact closely with certain symmetries. Secondly, collisions have

been used by Kambe and his co-workers primarily to test theories of vortex sound generation. Finally, McWilliams (1983) suggested that collisions may result in the discovery of new types of vortex solutions in the same way that particle collisions have led to the discovery of new particles. We think that this motivation is not too fanciful; we shall see below that from a vortex ring collision, there emerges a structure related to a stationary solution of the two-dimensional equations.

With perfect symmetry, each vortex can be regarded as the image of the other with respect to a slip wall, for example an uncontaminated free surface at Froude numbers so low that the surface does not deform (Bernal et al 1989). Let us consider the effects of core deformation and viscosity in turn. Oshima (1978) performed collisions at Re_D between 260 and 400, varied by increasing the level of electric current to a speaker; apparently the displacement of the driving speaker also increases since thicker cores are formed. For small cores, the smoke cross-sections deform from a circular to an airfoil shape as they collide. For thicker cores the core deformation is stronger. The dye forms a head with a long trailing tail. Subsequently, the head pinches off from the tail and continually increases in radius. At larger radii, azimuthal waviness occurs. Beautiful two-color photographs of Lim et al (1989) show that the waves pinch to form a dozen or so smaller rings.

Axisymmetric contour dynamics calculations (Shariff et al 1988, 1989) reveal some of the inviscid effects. Thin cores approach each other slowly compared to how fast they spin so the core shapes remain in equilibrium with respect to the slowly changing velocity field induced upon them by the other vortex. Their shapes evolve through the shapes of the family of steady translating two-dimensional vortex pairs of Pierrehumbert (1980) up to (almost) the touching member of the family. Energy conservation implies that the vorticity distribution cannot remain unchanged as the vortices stretch in radius $\bar{\sigma}$. (The energy of a vortex ring dipole $\sim \Gamma^2 \bar{\sigma}$ for a given vorticity distribution in the core.) One means of conserving energy is for the cores to become sheet-like, however, simulations indicate that this does not happen uniformly everywhere: The core retains the shape of a 2-D pair, which sheds vorticity into a sheet-like tail. For fat rings the strain-rate changes sufficiently rapidly such that the initial deformation is severe, but then there emerges a head with the shape of a steady 2-D pair with a trailing tail. The head-tail structure is also observed in symmetric interactions of three-dimensional vortex tubes (Pumir & Kerr 1987, Mclander & Hussain 1988).

In order to understand some effects of viscosity we turn to the numerical simulations of Kambe & Mya Oo (1984) and Stanaway et al (1988c). As in the inviscid case, a head-tail structure forms. For thin cores, the circulation

remains nearly constant initially and then decays as the cores "make contact" and gradients intensify at the collision plane. On the other hand, the energy decreases throughout.

For the reconnection of three-dimensional vortex tubes, out-of-plane strain accelerates annihilation of circulation (Schatzle 1987). Schatzle listed among many possible timescales, one (T_1) based upon a simple solution for one-dimensional vortex layers of opposite circulation pressed together by a strain-rate ε:

$$T_1 = \frac{1}{2\varepsilon} \log\left(\frac{\delta^2 \varepsilon}{\nu}\right), \tag{5.1}$$

which corresponded reasonably with his experiments. In the case of the head-on collision of rings, cores are pressed together at the rate

$$\varepsilon \approx \dot{\bar{\sigma}}/\bar{\sigma} \approx \Gamma/(4\pi\delta\bar{\sigma}), \tag{5.2}$$

which together with (5.1) predicts a timescale that agrees best with the simulation of Stanaway et al (1988c, Case 1) among those listed by Schatzle.

In their acoustic measurements for head-on collisions Kambe & Minota (1983) separated Möhring's (1978) quadrupole from a monopole contribution resulting from energy dissipation. It was believed that viscosity was required to explain the later form of the quadrupole wave; however, the results of Shariff et al (1988, 1989) suggest that inviscid core deformation is sufficient.

5.3 *Head-On Collision with a No-Slip Wall*

Consider the interaction of a wall and a vortex ring (with + vorticity say) moving normally towards it. Walker et al (1987) described the process using flow visualization experiments and analysis of the unsteady wall boundary layer. Professor P. Orlandi has kindly provided the results of some numerical calculations (see Figure 7) for which the trajectories of the rings agree well with the experiments and which aid the precision of the following description.

The boundary layer experiences an adverse pressure gradient in the regions outward from the radius of the ring. At sufficiently large Reynolds numbers this promotes separation of wall vorticity, which creates a secondary ring (−) bound to and orbitting about the primary ring (+). Meanwhile, the primary ring continues to create more vorticity of the opposite sign, which forms yet a tertiary (−) ring. At even larger Reynolds numbers, for example the case of Figure 7, the secondary ring becomes released from the primary and escapes away from the wall! Notice the role of

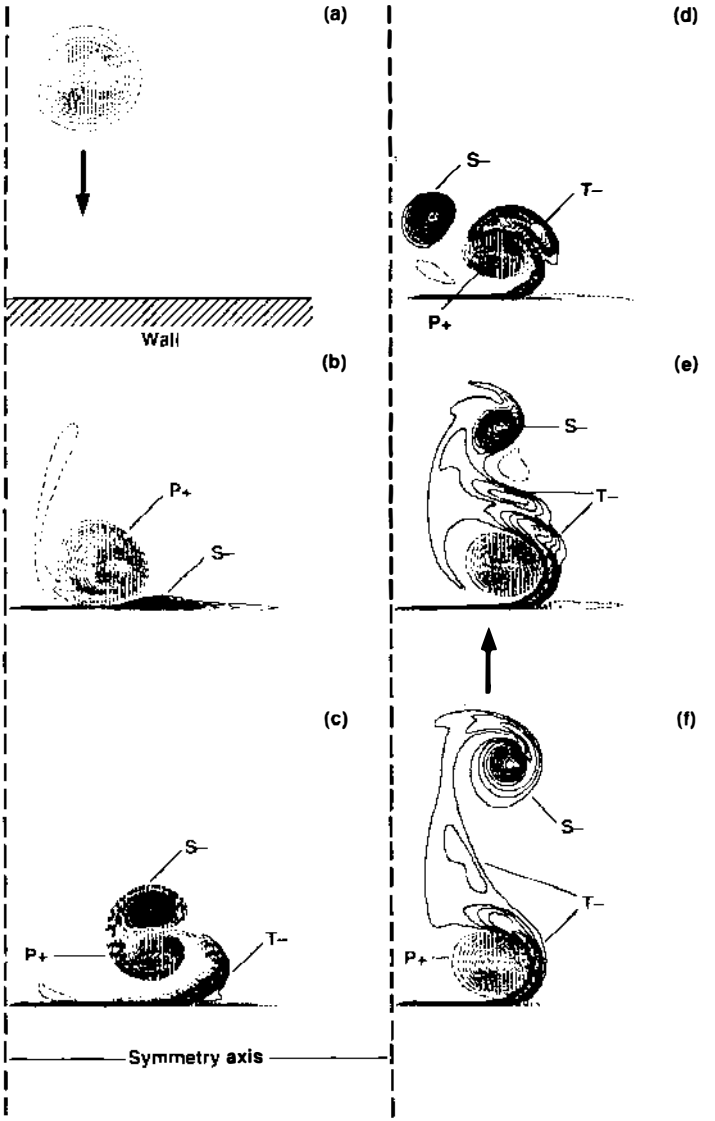

Figure 7 Courtesy of P. Orlandi. Vorticity contours for impingement of a vortex ring on a no-slip wall. ($\Gamma_0/\nu = 6577$, $Re_D \approx 2840$.) Dashed contours indicate positive vorticity. P, S & T denote primary, secondary and tertiary vorticity, respectively. $+/-$ indicates the sense of vorticity.

tertiary vorticity in causing the secondary to become unbound and then strengthened by pairing, thus enabling its escape.

6. AZIMUTHAL INSTABILITIES

Theoretical work of the late 1800s suggested that inviscid vortex rings are neutrally stable. For example, Kelvin (1880) showed that a rectilinear vortex with an initially circular core containing uniform vorticity could support a spectrum of neutrally stable modes of vibration. Analyses of vortex rings, carried up through terms of $\mathcal{O}(\delta/R)$ showed no instability. About half a century later, however, experiments began to suggest the possibility that rings that are well-formed at the orifice could undergo an instability to azimuthal waves (Krutzsch 1939, Maxworthy 1972). Perhaps in deference to the early theoreticians it was generally thought, at the time, that the observed instabilities were due to the generation process during which, for example, foreign matter or secondary vorticity was injected into the ring.

It is now known that the instabilities are for real. The correct theoretical explanation for them was developed only within the last 20 years. It is somewhat ironic that Kelvin's analysis for the neutral waves can be used as one of the ingredients to a simplified demonstration of the instability mechanism (Widnall et al 1974). The other ingredient is the effective straining field that is imposed on the vortex core because of the geometry of the ring. Figure 8 shows the orientation of the straining field. The

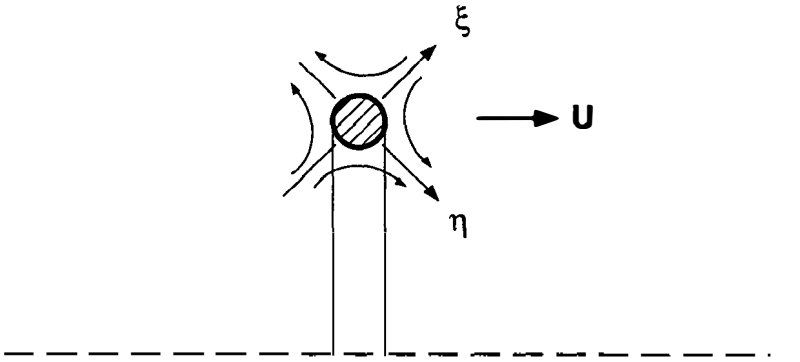

Figure 8 Cross-section of a vortex ring with speed U showing strain axes due to curvature.

magnitude of the strain-rate ε is $\mathcal{O}[\Gamma/R^2 \log(R/\delta)]$. In Figure 9 we show the rotation rate Ω versus axial wavenumber of various neutrally stable modes of bending on a rectilinear vortex (after Kelvin). Adding the straining field due to the filament curvature, one can approximate the dynamics of the peak amplitude (ξ_p, η_p) in the cross plane (Widnall et al 1974, Moore & Saffman 1975a) as

$$\frac{d\xi_p}{dt} = \Omega\eta_p - \varepsilon\xi_p,$$

$$\frac{d\eta_p}{dt} = -\Omega\xi_p + \varepsilon\eta_p. \tag{6.1}$$

For $\varepsilon^2 > \Omega^2$ one obtains an instability

$$\xi_p, \eta_p \sim \exp(\sqrt{\varepsilon^2 - \Omega^2}\, t). \tag{6.2}$$

The requirement that an integer number of waves exist on the ring ($k = N/R$) gives a discrete set of allowable ks. From an inviscid standpoint, the radial mode that has the minimum absolute rotation rate over the

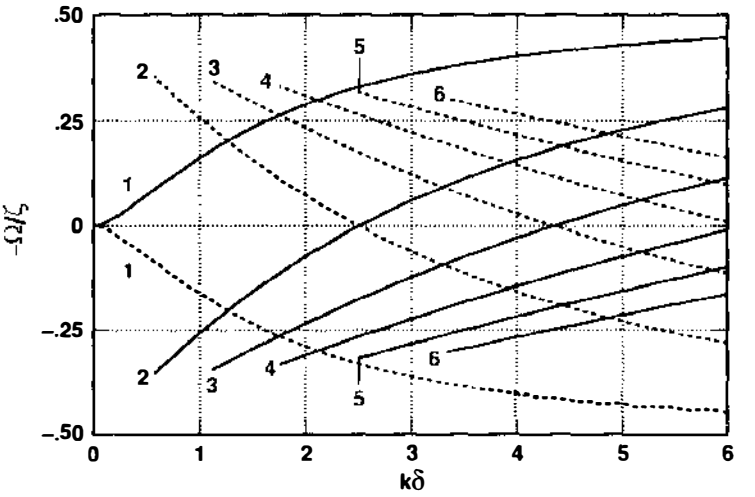

Figure 9 Rotation rate Ω for helical waves of bending ($|m| = 1$) on a rectilinear vortex with uniform vorticity ζ (after Kelvin 1880). The waves are of the form $\exp[i(-\Omega t + m\theta + kx)]$. The numerals beside each curve are labels for the radial structure of the corresponding eigenfunction. The solid and dashed curves correspond to opposite senses of twist: $m = +1$ and $m = -1$, respectively.

discrete set of ks would correspond to the most amplified wavy mode on the ring.[2] However viscous effects will likely favor the mode that has the least radial structure (Widnall et al 1974). This mode is labelled *2* in Figure 9 and is called the second radial mode.

Experimental evidence supports the above proposal. Maxworthy (1977) confirmed that during the small amplitude phase, stagnant (nonrotating and nonpropagating) waves grow at 45° relative to the direction of ring propagation. At large amplitudes, the waves begin to rotate and the core fluid is mixed and becomes turbulent. That it is the second radial mode that appears is seen in Plate 114 of Van Dyke's (1982) album. Focusing on a cross-section at which the inner core (the darkest portion of dye) moves outward, one observes that the outward portions of the core are displaced inward so that a profile of the eigenfunction for radial velocity has one zero crossing within the core.

Theoretical confirmation of the instability came with the work of Widnall & Tsai (1977) who determined that a thin vortex ring with a core of constant vorticity is indeed unstable by an analysis including terms up through $\mathcal{O}(\delta^2/R^2)$. To obtain good agreement with experiment one should use more realistic vorticity profiles in the stability calculation. As discussed in Section 2.2, Saffman (1978), using a vortex sheet roll-up model, predicted the vorticity distributions for a series of ring experiments by Leiss and Didden. Compared with experiment the agreement for the number of waves from the subsequent stability analysis was excellent.

Some important related issues remain unresolved, however. What are the events succeeding the development of the azimuthal waves during the linear amplification stage, leading to transition to turbulence? What characterizes the instantaneous vortical structure of a turbulent vortex ring? At this time we have only meager bits of sometimes conflicting experimental evidence to help answer these questions. Sturtevant (1981) found that the azimuthal waviness decayed and vanished while Maxworthy (1977) observed that the waves break and, therafter, a rapidly propagating wave of core diameter pulsation creates flow in the azimuthal direction. It is conjectured that the axial flow occurs because waves do not break at different azimuthal locations at the same time. It has been suggested that axial flow prevents further instability since the resulting turbulent vortex is apparently stable. From the flow visualization part of their investigation of turbulent rings, Glezer & Coles (1990) suggest that secondary vortex tubes are wrapped around the main core, alternating in sign of circulation.

[2] As pointed out by Moore & Saffman (1975a), the concept of a "radial mode" has to be generalized to include the possibility of a superposition of two eigenmodes of the same axial wavenumber and rotation rate but different radial structure and opposite sense of twist. These correspond to the intersection of solid and dashed curves in Figure 9.

7. TURBULENT VORTEX RINGS AND PUFFS

7.1 *Classification*

Of the simple turbulent shear flows listed in Table 2 of the review by Cantwell (1981), among the least understood are the turbulent vortex ring and puff. They can be described as a compact turbulent region with net linear momentum, statistically invariant with respect to rotation about one axis; one type of mean that can therefore be used is the average over the azimuthal direction. Such flows offer many features to interest and challenge a turbulence researcher: mean rotation and streamline curvature, a time evolving mean, and a growing interface between turbulent and nonturbulent flow.

A wide range of structure is subsumed by the definition above and one would like to begin by listing the measurable parameters that are seen to affect the observables, currently the growth-rate. But as attested by the attempts of Maxworthy (1977, his Section 5) this seems very difficult at present. For example, one important parameter is probably the ratio of space integrated rms fluctuation velocity to the linear impulse; a realization having a small value of this parameter would have a smaller growth rate. However this parameter is not easily measurable and sudden changes in growth rate (Maxworthy 1977, Brasseur 1979) remind one that structure parameters can dramatically change in this unusual flow. Consequently, we shall be content to distinguish between three types of structures depending on how they are generated. There are two kinds of turbulent rings, those in which the turbulence initiates naturally at the vortex generator (Section 2.3) and those that begin as laminar and undergo transition via an azimuthal instability some distance after formation; differences between characteristics of the two types is a matter requiring study. The third type is the turbulent puff, which is produced by placing gauze or a perforated plate at the pipe exit.

7.2 *Flow Visualization Studies of Turbulent Rings*

Currently the primary source of information about processes in a turbulent vortex ring is flow visualization experiments. A parallel series of tests was conducted by Maxworthy (1974) and Vladimirov & Tarasov (1979); in the former case it is stated that the rings became turbulent via an azimuthal instability. First, a blob of dye expelled with the ring becomes corrugated, clear fluid is entrained and mixes with the dye and the mixture is shed into a wake; eventually dye is left only in a thin slowly growing toroidal core. Next, an initially unmarked ring is pushed through a patch of dye; a blob of fluid becomes dyed except for a thin toroidal core,

which remains clear. The blob sheds a mixture of dye and clear fluid and eventually only the outer edge of the core remains dyed. These features are also true of rings that are turbulent at the generator (A. Glezer, private communication).

Since convective transport of vorticity from the core is evidently small compared to the influx of irrotational fluid into the bubble, it is probably true that a substantial fraction of the vorticity is confined to a thin toroidal core. Modes of unsteadiness around the core or in the azimuthal direction, would by their Biot-Savart induced velocity, entrain ambient irrotational fluid and detrain weakly vortical fluid into the wake of the ring. Low-order modes of the vorticity are most efficient in contributing to this process because the Biot-Savart velocity induced by higher-order modes decays faster with distance from the core. This is consistent with the observation of Maxworthy (1974) that "major motions in the outer bubble are of larger scale." To illustrate one aspect of this process we consider the simple unsteadiness exhibited by the axisymmetric elliptical core vortex ring solution of Moore (1980). Tools from dynamical systems theory can be used to provide information about the rate of fluid engulfment and rejection from the vortex bubble in each period of the unsteadiness. Figure 10

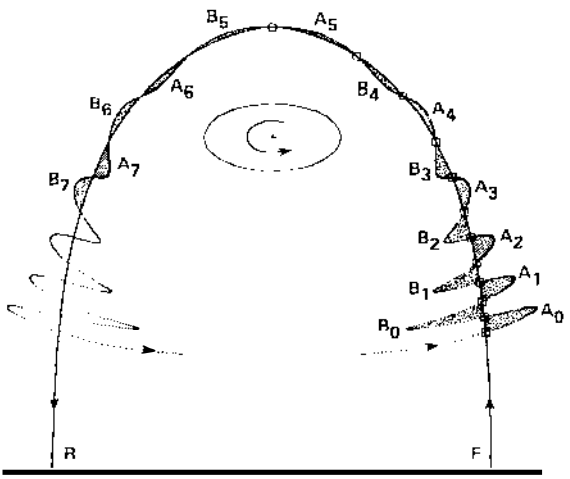

Figure 10 From Shariff et al (1989). Abridged stable and unstable manifolds for an elliptic core ring, illustrating fluid engulfment and rejection from the vortex ring bubble. The bubble is well defined here as the curved region FR.

(Shariff et al 1989) shows the motion of ambient fluid in lobe A_0 as it travels from one period to the next. It is entrained into the vortex bubble as lobe A_6, after which it is stretched into a thin streak. Such streaks are present in those studies of Maxworthy (1974) and Sturtevant (1981), which employ slight density contrast to visualize the bubble fluid. Similarly, region B_0 in Figure 10 is detrained from the bubble as region B_5. Observed corrugations of the dye interface are probably a result of a process like this. Eventually some iterate of the entrained region A_7 will have a portion lying in B_5, i.e. some portion will be detrained. Notice the large straining of the detrained fluid; in a three-dimensional flow with weak vorticity present in the bubble (Maxworthy 1977), this process would lead to intensification of streamwise vorticity.

The process described above represents an exchange of ambient and bubble fluid but does not account for net permanent entrainment. Maxworthy's (1974) view is essentially the one above but in addition emphasizes the fact that the core also entrains fluid but at a slower rate. This process accompanies the slow growth of the size of the ring. Maxworthy also observes loss of vorticity from the core and this forms the basis of a scaling theory, which we shall discuss later.

Corrugations of the dye interface have sometimes been compared to a shear layer instability, entrainment is described as taking place through a shear layer at the bubble boundary, streaky features in the bubble have been described as fully developed turbulence, and loops of dye in the wake of the ring are interpreted as being hairpin vortices or as arising from a Görtler instability. Given that unsteadiness of the core can account for irrotational dye motions similar to those observed in experiments means that careful evidence must be gathered before those motions are said to be vortical. For example Glezer & Coles (1990) presented views of fluorescent dye in various planes normal to the symmetry axis. Their interpretation that streamwise vorticity is present is plausible only because of nonzero radial normal Reynolds stress behind the ring (Figure 11). If confident statements about the vorticity are to be made, dye should be placed only in the vortical shear layer when the ring is generated, and secondly, dye should not be placed nonaxisymmetrically as it can form three-dimensional loops even in an axisymmetric flow.

The viewpoint that core unsteadiness must drive the processes of entrainment and detrainment and possibly the formation of secondary vorticity should lead one to inquire about processes that occur in the core. With the observation that a dye spiral injected at a particular azimuthal location maintained its identity for large distances, Vladimirov & Tarasov (1979) concluded that turbulence is suppressed in the core but is sustained outside.

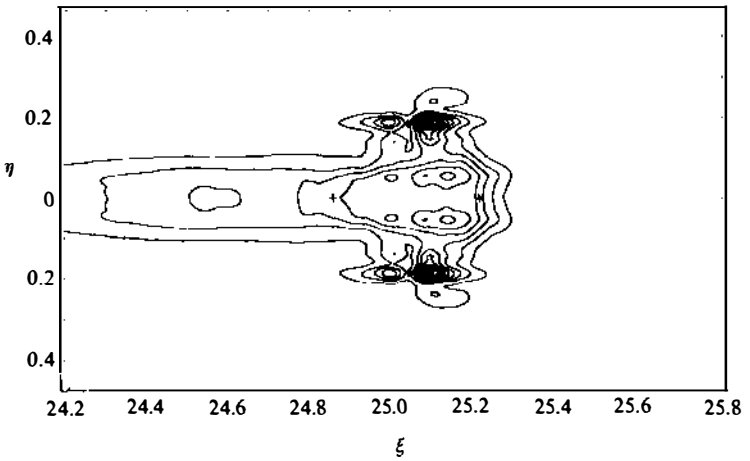

Figure 11 From Glezer & Coles (1990). Experimental measurement of the radial normal Reynolds stress, $\langle u'_r u'_r \rangle (\rho/I)^{1/2}(t-t_0)^{3/2}$, in similarity coordinates.

This is supported by Glezer & Coles (1990, p. 276) whose measurements indicate lower turbulent stresses in the inner core region. Occasional suggestions about the suppression of turbulence in vortex cores have appeared in other contexts as well: for the turbulent vortex pair in Barker & Crow (1977) and for the turbulent trailing vortex in Bandyopadhyay et al (1990). Probably the most curious observation of visualization of the core is the presence of a single wave of expansion on the core, which propagates in the direction of the vorticity and induces an axial flow in the azimuthal direction (Maxworthy 1977). It is observed only at high Re_p and its inception seems to be a result of nonuniform breaking of instability waves. Both of the results quoted here were made possible through selective tagging of fluid regions. Today, with the availability of fluorescent and photochromic dyes, the possibilities for investigating core dynamics have greatly expanded.

7.3 *Scaling Behavior*

If one assumes that after some development, the evolution of a statistical quantity— the mean axial velocity $\bar{u}_x$ say—becomes independent of kinematic viscosity and diameter of the vortex generator and depends only on the linear impulse I/ρ, then from dimensional analysis (Glezer & Coles 1990)

$$\frac{\bar{u}_x}{\bar{u}_s} = f(\xi, \eta),$$

$$\bar{u}_s \equiv (I/\rho)^{1/4}(t-t_0)^{-3/4} \text{ (a velocity scale)},$$

$$\xi \equiv (x-x_0)\left(\frac{\rho}{(t-t_0)I}\right)^{1/4},$$

$$\eta \equiv \sigma\left(\frac{\rho}{(t-t_0)I}\right)^{1/4}. \tag{7.1}$$

In these expressions x_0 and t_0 are virtual origins. The value of $\bar{u}_x$ at a point (ξ_0, η_0) fixed in similarity coordinates is propagated in physical space along a line with slope η_0/ξ_0 and with axial speed $\sim(t-t_0)^{-3/4}$. The fact that the far-field velocity cannot decay in time provides a constraint on the behavior of $f(\xi, \eta)$ as $\xi, \eta \to \infty$.

These relations imply that the mean circulation decays as $\bar{\Gamma} \sim t^{-1/2}$ and this can only occur by viscous or turbulent flux of oppositely signed vorticity across the symmetry axis. The above scaling laws can be obtained in a number of other ways. For instance early work on puffs (Grigg & Stewart 1963, Richards 1965) used the experimental observation of the conical nature of the flow ($R \sim X$) together with the requirement of conservation of impulse.

The evidence for or against the realization of self-similarity is not overwhelming. Accepting some scatter and oscillations in the data, most experiments indicate that conical growth is present but with a notable twist in some observations of turbulent rings: The growth rate can change to a different value downstream. This transition appears to be present in the data of Sallet & Widmayer (1974) at about 35 diameters of travel and is explicitly pointed out and studied by Maxworthy (1977). Two types of evidence exist for the scaling of the velocity. First, one has plots such as $U^{-1/3}$ against x. Here U is the propagation velocity from dye observations or peak velocities of mean hot-wire traces at the symmetry axis. One must be very self-critical in attempting to fit power-laws to the data since a plot of $U^{-1/p}$ as a function of $x-x_0$ with x_0 as a free parameter can provide reasonable straight line fits for a wide range of p; one should obtain rather the best value of p that fits the data and, if possible, obtain x_0 independently. The small growth rate of the vortex ring implies large negative virtual origins and large errors in its determination. Johnson (1970, 1971) shows that his data fits both the self-similar forms as well as a different set of power laws. The second piece of evidence is the fairly good collapse at several axial stations of suitably averaged velocity profiles at the symmetry axis (Glezer & Coles 1990).

Maxworthy (1974) has put forward an alternative to the impulse based self-similarity hypothesis. Attention is focused on the vortical core and the fluid transported with it. The core loses vorticity either by pieces of it being torn-off or through viscous diffusion (Maxworthy 1977). This vorticity is carried into the bubble and subsequently detrained into the wake and thereafter becomes unimportant in affecting the bubble or core dynamics. Now the speed of the ring and how much fluid it carries with it is determined by the properties of the dynamically active vortical core. It therefore makes sense to define an impulse-like quantity I' proportional to ρVU, where V is the volume of the bubble. The hypothesis is that loss of vortical fluid causes I' to decrease as

$$\frac{dI'}{dt} = -\frac{1}{2} C_D'' \rho U^2 \pi R^2 k, \tag{7.2}$$

where C_D'' is a coefficient analogous to the drag coefficient of a solid body and k is a shape parameter. Together with the entrainment hypothesis, which states that the rate of increase of bubble volume is proportional to bubble surface area and velocity (equivalent to the assumption of conicality), one obtains

$$U = D_1(x - x_0)^{-(C_D+3)}, \tag{7.3a}$$

$$U = D_2(t - t_0)^{-(C_D+3)/(C_D+4)}. \tag{7.3b}$$

For $C_D = 0$ one recovers the result of the similarity theory. After determining the virtual origin from the R data, Maxworthy (1974) plots U vs $(x - x_0)$ in log-log coordinates and obtains values of C_D as large as 2.7!

Consider the dependence of spreading angle $\alpha' = (X - X_0)/R$ on apparatus parameters L/D and Re_p. In 1977 Maxworthy abandoned his earlier view that α' was universal and studied its dependence on both apparatus parameters (see his Table 1). Perrakis & Papailiou (1988) studied the effect of Re_p on α' and Glezer & Coles (1990, Table 3) compiled additional data. Disappointingly, no consistent trend emerges. We might naively expect thinner cores to have larger α' because their core dynamics are more rapid compared to forward translation. However, upon observing behavior over a larger range of Re_p than contained in his table, Maxworthy concluded that fatter cores had the larger growth rate and proposed that thinner cores may have different core organization, for example, they may be stabilized by axial flow.

7.4 *Mean Structure*

Although azimuthal averages would be more revealing of the dynamics, current experiments obtain ensemble averages. Perhaps because mean

rotation diminishes variations in the azimuthal directions there is considerably more dispersion in the properties of individual realizations; this point emphasized by Glezer & Coles (1990) means that the ensemble average is not the same as the azimuthal average.

Kovasznay et al (1974) assumed that the mean flow is governed by the linear Stokes equation with a spatially uniform but time-dependent turbulent viscosity proportional to the product of an evolving velocity and length scale of the solution itself. Since rms velocity fluctuations decay as r^{-3} (or faster) in the potential far-field and mean gradients decay as $1/r^4$, the eddy viscosity cannot be uniform. However, measurements in other flows such as jets (Hinze 1975, p. 537) show that within the turbulent region the eddy viscosity is fairly constant and decays in the free-stream. Solutions of the equation formulated by Kovasznay et al follow the self-similarity scalings and the least decaying solution in time for the mean flow is identical to Phillips (1956) decaying vortex ring solution discussed in Section 3.3 with only time transformed. While the ensemble averaged velocity field measured by Kovasznay et al for turbulent puffs followed in general the scaling behavior, its structure failed to conform to the theoretical solution. One can only speculate that constant eddy viscosity is more appropriate for the azimuthal mean than the ensemble mean. In 1969 Lugovtsov et al (see Lugovtsov 1976) formulated a model based on an identical assumption for the eddy viscosity but retained the nonlinear term of the mean flow and cast the equations in similarity variables; however no solutions were provided. One thus has a situation that is singular in the study of turbulent shear flows in which even a fair agreement of the measured and modeled mean flow is lacking.

Glezer & Coles (1990) have devoted considerable effort towards dealing with the problem of dispersion and of extracting meaningful averages from ensemble measurements. They provide for the first time measurements at one axial station of mean velocities, vorticity, and turbulent stresses, plotted in similarity coordinates (ξ, η). Figure 11 shows the radial normal Reynolds stress; it dips in the center of the core and of all the turbulent stresses (for velocity components in the meridional plane) it is the only one with a "wake," suggesting axial vorticity.

7.5 *Recommendations*

We hope that as multi-point velocimetry techniques mature the need to rely on ensembles will disappear.

It is possible for thin cores that curvature effects—namely, vortex stretching and strain due to curvature—can be neglected in the core. In this case self-preserving solutions have the circulation as the invariant parameter and the core size grows as $t^{1/2}$, core velocities decay as $t^{-1/2}$,

while outer flow velocities decay as $\log(1/t)$. One may therefore wish to inquire as to the importance of curvature effects by observing the degree to which turbulent stresses of velocity components, in polar coordinates centered at the core, are functions of the radial distance only.

In Section 4 of his paper Maxworthy (1977) initiated a useful method of attack—namely, that of introducing controlled perturbations to understand a specific aspect of the problem. In addition to those he considered, we would like to suggest axisymmetric straining by passing the ring through a large converging tube and nonaxisymmetric straining by changing the cross-section through which the ring propagates.

There are encouraging prospects for numerical simulations in this area. At the simplest level inviscid vortex filament calculations employing very many degrees of freedom may be useful. Inoue (1988) has performed such calculations aimed at studying transition, and while his solutions depict core growth there is reason to believe that it is due to amplitude error of the time integration scheme. Such a simulation should attempt to retain vortex elements in the weak vorticity region, which may subsequently be stretched. Another possibility is the use of spectral methods in an unbounded domain as initiated by Stanaway et al (1988a,b).

Other parts of this review have discussed the use of vortex rings in "clean" aeroacoustic experiments to understand basic mechanisms of sound generation. Zaitsev et al (1990) have made preliminary measurements of the sound field of a turbulent vortex ring. Spectra are peaked at a frequency such that the Strouhal number $2fR/U \approx 1.9$ initially; the peak frequency decays downstream. Assuming that the most efficient sound sources are low-order modes of core vibration, we tried to fit the initial measured frequency to two contenders: the elliptic azimuthal mode [see Equation (35) in Widnall & Sullivan (1973) for the frequency] and Moore's (1980) axisymmetric elliptic core ring. The former fits the data for the unrealistically large value of $\delta/R \approx 3$, while the axisymmetric mode fits the data for a more reasonable value of $\delta/R \approx 0.3$; further measurements, of the directivity pattern say, should yield more definitive proof. In this context, it is relevant that Auerbach (1991) reports, for experiments at smaller Reynolds numbers, that Strouhal numbers associated with periodic ejections of dye from the recirculation bubble were in the range of 2 to 4.

Literature Cited

Akhmetov, D. G. 1980. Extinguishing gas and oil well fires by means of vortex rings. *Combust. Explos. Shock Waves* 16: 490–94

Allen, G. A. Jr. 1984. *Transition and mixing in axisymmetric jets and vortex rings.* PhD thesis, Stanford Univ. Also, *Report SUDAAR 541*, Dept. Aeronautics, Stanford Univ., Stanford, Calif.

Auerbach, D. 1987. Experiments on the trajectory and circulation of the starting vortex. *J. Fluid Mech.* 183: 185–98

Auerbach, D. 1988. Some open questions on the flow of circular vortex rings. *Fluid Dyn. Res.* 3: 209–13

Auerbach, D. 1991. Stirring properties of vortex rings. *Phys. Fluids A* 3: 1351–55

Bandyopadhyay, P., Stead, D., Ash, R. 1990. The organized nature of a turbulent trailing vortex. *AIAA Pap. No. 90–1625*

Barker, S. J., Crow, S. C. 1977. The motion of two-dimensional vortex pairs in ground effect. *J. Fluid Mech.* 82: 659–71

Batchelor, G. K. 1956. A proposal concerning laminar wakes behind bluff bodies at large Reynolds number. *J. Fluid Mech.* 1: 388–98

Batchelor, G. K. 1967, 1973. *An Introduction to Fluid Dynamics*. Cambridge: Cambridge Univ. Press

Batishchev, V. A., Srubshchik, L. S. 1971. Diffusion of a spherical Hill vortex with vanishing viscosity. *Sov. Phys. Dokl.* 16: 286–88

Benjamin, T. B. 1962. Theory of the vortex breakdown phenomenon. *J. Fluid Mech.* 14: 593–629

Benjamin, T. B. 1976. The alliance of practical and analytical insights into the nonlinear problems of fluid mechanics. In *Applications of Methods of Functional Analysis to Problems in Mechanics*, P. Germain, B. Nayroles, Lecture Notes in Mathematics, 503: 8–28. New York: Springer

Bernal, L. P., Hirsa, A., Kwon, J. T., Willmarth, W. W. 1989. On the interaction of vortex rings and pairs with a free surface for varying amounts of surface active agent. *Phys. Fluids A* 1: 2001–4

Brasseur, J. G. 1979. *Kinematics and Dynamics of Vortex Rings in a Tube.* PhD thesis. Stanford Univ.

Cantwell, B. J. 1981. Organized motion in turbulent flow. *Annu. Rev. Fluid Mech.* 13: 457–515

Cantwell, B. J. 1986. Viscous starting jets. *J. Fluid Mech.* 173: 159–89

Cantwell, B. J., Rott, N. 1988. The decay of a viscous vortex pair. *Phys. Fluids* 31: 3213–24

Chahine, G. L., Genoux, P. F. 1983. Collapse of a cavitating vortex ring. *J. Fluids Eng.* 105: 400–5

Chapman, D. S., Critchlow, P. R. 1967. Formation of vortex rings from falling drops. *J. Fluid Mech.* 29: 177–85

Chen, C.-J., Chang, L.-M. 1972. Flow patterns of a circular vortex ring with density differences under gravity. *J. Appl. Mech.* 39: 869–72

Couder, Y., Basdevant, C. 1986. Experimental and numerical study of vortex couples in two-dimensional flows. *J. Fluid Mech.* 173: 225–51

Crighton, D. G. 1980. Jet noise and the effects of jet forcing. In *The Role of Coherent Structures in Modelling Turbulence and Mixing*, ed. J. Jimenez, Lecture Notes in Physics, 136: 340–62. New York: Springer

Dabiri, D., Gharib, M. 1991. Digital particle image thermometry and its application to a heated vortex ring. *Exp. Fluids* 11: 77–86

Didden, N. 1979. On the formation of vortex rings: Rolling-up and production of circulation. *J. Appl. Mech. Phys.* (*ZAMP*) 30: 101–16

Didden, N. 1982. On vortex formation and interaction with solid boundaries. In *Vortex Motion*, ed. H. G. Hornung, E.-A. Müller, pp. 1–17. Braunschweig/Wiesbaden: Friedr. Vieweg. & Sohn

Dimotakis, P. E. 1984. Entrainment into a fully developed two-dimensional shear layer. *AIAA Pap. No. 84-0368*

Durst, F., Schönung, B. 1982. Computations of steady ellipsoidal vortex rings with finite cores. *Comput. Fluids* 10: 87–93

Dyson, F. W. 1893. The potential of an anchor ring—Pt. II. *Philos. Trans. R. Soc. London Ser. A* 184: 1041–1106

Eydeland, A., Turkington, B. 1988. A computational method of solving free-boundary problems in vortex dynamics. *J. Comput. Phys.* 78: 194–214

Fetter, A. 1974. Translational velocity of a classical vortex ring. *Phys. Rev. A* 10: 1724–27

Fornberg, B. 1988. Steady viscous flow past a sphere at high Reynolds numbers. *J. Fluid Mech.* 190: 471–89

Fraenkel, L. E. 1972. Examples of steady vortex rings of small cross-section in an ideal fluid. *J. Fluid Mech.* 51: 119–35

Fraenkel, L. E., Berger, M. S. 1974. A global theory of steady vortex rings in an ideal fluid. *Acta Math.* 132: 13–51

Glezer, A. 1988. The formation of vortex rings. *Phys. Fluids A* 31: 3532–42

Glezer, A., Coles, D. 1990. An experimental study of a turbulent vortex ring. *J. Fluid Mech.* 211: 243–83

Grigg, H. R., Stewart, R. W. 1963. Turbulent diffusion in a stratified fluid. *J. Fluid Mech.* 15: 174–86

Helmholtz, H. 1858. *On integrals of the hydrodynamical equations which express vortex-motion.* Transl. P. G. Tait, 1867 with a letter by Lord Kelvin (W. Thomson), in *London Edinburgh Dublin Phil. Mag. J. Sci.* Fourth series 33: 485–512 (From German)

Hill, M. J. M. 1894. On a spherical vortex. *Philos. Trans. R. Soc. London Ser. A* 185: 213–45

Hinze, J. O. 1975. *Turbulence.* New York: McGraw-Hill

Hussain, A. K. M. F., Zaman, K. B. M. Q. 1980. Vortex pairing in a circular jet under controlled excitation. Part 2. Coherent structure dynamics. *J. Fluid Mech.* 101: 493–544

Inoue, O. 1988. Simulation of a vortex ring. *AIAA Pap. No. 88-3571-CP*

Johari, H. 1990. Flame length measurements of turbulent vortex rings. *Bull. Am. Phys. Soc.* 35: 2287

Johnson, G. M. 1970. Researches on the propagation and decay of vortex rings. *ARL Rep. 70-0093*, Aerospace Res. Labs., Wright-Patterson Air Force Base, Ohio

Johnson, G. M. 1971. An empirical model on the motion of turbulent vortex rings. *AIAA J.* 9: 763–64

Kaden, H. 1931. *Curling of an unstable discontinuity interface.* Transl. 1972, NASA Tech. Transl. TT F-14,230 (From German)

Kambe, T. 1984. Axisymmetric vortex solution of the Navier-Stokes equation. *J. Phys. Soc. Jpn.* 53: 13–15

Kambe, T., Minota, T. 1983. Acoustic wave radiated by head-on collision of two vortex rings. *Proc. R. Soc. London Ser. A* 386: 277–308

Kambe, T., Oshima, Y. 1975. Generation and decay of viscous vortex rings. *J. Phys. Soc. Jpn.* 38: 271–80

Kambe, T., Mya Oo, U. 1984. An axisymmetric viscous vortex motion and its acoustic emission. *J. Phys. Soc. Jpn.* 53: 2263–73

Kelvin, Lord (Thomson, W.) 1880. Vibrations of a columnar vortex. *London Edinburgh Dublin Phil. Mag. J. Sci.* Fifth series 10: 155–68

Kop'ev, V. F., Leont'ev, E. A. 1988. Acoustic instability of planar vortex flows with circular streamlines. *Sov. Phys. Acoust.* 34: 276–78

Kovasznay, L. S. G., Fujita, H., Lee, R. L. 1974. Unsteady turbulent puffs. *Adv. Geophys.* 18B: 253–63

Krasny, R. 1987. Computation of vortex sheet roll-up in the Trefftz plane. *J. Fluid Mech.* 184: 123–55

Krutzsch, C.-H. 1939. Über eine experimentell beobachtete Erscheinung an Wirbelringen bei ihrer translatorischen Bewegung in wirklichen Flüssigkeiten. *Ann. Phys.* 35: 497–523

Küchemann, D. 1965. Report on the I.U.T.A.M. symposium on concentrated vortex motions in fluids. *J. Fluid Mech.* 21: 1–20

Lamb, Sir H. 1932. *Hydrodynamics.* New York: Dover

Leith, C. E. 1984. Minimum enstrophy vortices. *Phys. Fluids* 27: 1388–95

Leonard, A. 1985. Computing three-dimensional incompressible flows with vortex elements. *Annu. Rev. Fluid Mech.* 17: 523–59

Lim, T. T., Nickels, T. B., Chong, M. S. 1989. A note on the cause of rebound in vortex ring/wall interactions. In *Proc. 10th Australasian Fluid Mech. Conf.*, pp. 10.11–14. Univ. Melbourne

Lugovtsov, B. A. 1976. On the motion of a turbulent vortex ring. *Arch. Mech. Stosowanei* 28: 759–76

Lundgren, T. S., Mansour, N. N. 1991. Vortex ring bubbles. *J. Fluid Mech.* 224: 177–96

Lundgren, T. S., Yao, J., Mansour, N. N. 1991. Microburst modelling and scaling. Submitted to *J. Fluid Mech.*

Maxworthy, T. 1972. The structure and stability of vortex rings. *J. Fluid Mech.* 51: 15–32

Maxworthy, T. 1974. Turbulent vortex rings (with an appendix on an extended theory of laminar vortex rings). *J. Fluid Mech.* 64: 227–39

Maxworthy, T. 1977. Some experimental studies of vortex rings. *J. Fluid Mech.* 81: 465–95

Maxworthy, T. 1979. Comments on "Preliminary study of mutual slip-through of a pair of vortices." *Phys. Fluids* 22: 200

McWilliams, J. 1983. Interactions of isolated vortices. II. Modon generation by monopole collision. *Geophys. Astrophys. Fluid Dyn.* 24: 1–22

McWilliams, J. C. 1984. The emergence of isolated coherent vortices in turbulent flow. *J. Fluid Mech.* 146: 21–43

Melander, M. V., Hussain, F. 1988. Cut-and-connect of two anti-parallel vortex tubes. *Proc. 1988 Summer Program*, pp. 257–86. NASA Ames/Stanford Ctr. Turbulence Res., Stanford, Calif.

Melander, M. V., Zabusky, N. J., Styczek, A. S. 1986. A moment model for vortex interactions of the two-dimensional Euler equations. Part 1. Computational validation of a Hamiltonian elliptical representation. *J. Fluid Mech.* 167: 95–115

Melander, M. V., Zabusky, N. J., McWilliams, J. C. 1988. Symmetric vortex merger in two dimensions: Causes and conditions. *J. Fluid Mech.* 195: 303–40

Minahen, C. D. 1983. *Hermeneutics of the vortex-structure in symbolist aesthetics: Phenomenology of a symbol as a symbol.* PhD thesis, Dept. Fr. Ital., Stanford Univ.

Minota, T., Kambe, T., Murakami, T. 1988. Acoustic emission from interaction of a vortex ring with a sphere. *Fluid Dyn. Res.* 3: 357–62

Moffatt, H. K. 1969. The degree of knottedness of tangled vortex lines. *J. Fluid Mech.* 35: 117–29

Moffatt, H. K., Moore, D. W. 1978. The

response of Hill's spherical vortex to a small axisymmetric disturbance. *J. Fluid Mech.* 87: 749–60

Moffatt, H. K. 1986. On the existence of localized rotational disturbances which propagate without change of structure in an inviscid fluid. *J. Fluid Mech.* 173: 289–302

Moffatt, H. K. 1988. Generalised vortex rings with and without swirl. *Fluid Dyn. Res.* 3: 22–30

Möhring, W. 1978. On vortex sound at low Mach Number. *J. Fluid Mech.* 85: 685–91

Moore, D. W. 1976. The stability of an evolving two-dimensional vortex sheet. *Mathematika* 23: 35–44

Moore, D. W. 1980. The velocity of a vortex ring with a thin core of elliptical cross-section. *Proc. R. Soc. London Ser. A* 370: 407–15

Moore, D. W. 1985. The effect of compressibility on the speed of propagation of a vortex ring. *Proc. R. Soc. London Ser. A* 397: 87–97

Moore, D. W., Saffman, P. G. 1972. The motion of a vortex filament with axial flow. *Philos. Trans. R. Soc. London Ser. A* 272: 403–29

Moore, D. W., Saffman, P. G. 1973. Axial flow in laminar trailing vortices. *Proc. R. Soc. London Ser. A* 333: 491–508

Moore, D. W., Saffman, P. G. 1975a. The instability of a straight vortex filament in a strain field. *Proc. R. Soc. London Ser. A* 346: 413–25

Moore, D. W., Saffman, P. G. 1975b. The density of organized vortices in a turbulent mixing layer. *J. Fluid Mech.* 69: 465–73

Müller, E.-A., Obermeier, F. 1988. Vortex sound. *Fluid Dyn. Res.* 3: 43–51

Norbury, J. 1973. A family of steady vortex rings. *J. Fluid Mech.* 57: 417–31

O'Brien, V. 1961. Steady spheroidal vortices—more exact solutions to the Navier-Stokes equations. *Q. Appl. Math.* 19: 163–68

Oguz, H. N., Prosperetti, A. 1989. Surface-tension effects in the contact of liquid surfaces. *J. Fluid Mech.* 203: 149–71

Oshima, Y. 1978. Head-on collision of two vortex rings. *J. Phys. Soc. Jpn.* 44: 328–31

Oshima, Y., Kambe, T., Asaka, S. 1975. Interaction of two vortex rings moving along a common axis of symmetry. *J. Phys. Soc. Jpn.* 38: 1159–66

Perrakis, K. K., Papiliou, D. D. 1988. Turbulent vortex ring entrainment mechanism. *Proc. Fifth Beersheba Intl. Seminar on Magnetohydrodynamics Flow and Turbulence*, pp. 105–15. Washington, DC: Am. Inst. Aeronaut. Astronaut.

Phillips, O. M. 1956. The final period of decay of non-homogeneous turbulence. *Proc. Cambridge Phil. Soc.* 52: 135–51

Pierrehumbert, R. T. 1980. A family of steady, translating vortex pairs with distributed vorticity. *J. Fluid Mech.* 99: 129–44

Poppe, W. 1978. Theoretische Untersuchung stationärer Ringwirbelströmungen mit unstetiger Wirbelstärkenverteilung. *Report 29/1978*, Max-Planck-Inst. Strömungsforschung, Göttingen, Germany

Poppe, W. 1980. Eine Schar von Ringwirbeln mit unstetiger Wirbelstärkenverteilung. *Z. Angew. Math. Mech.* 60: T209–10

Pozrikidis, C. 1986. The non-linear instability of Hill's vortex. *J. Fluid Mech.* 168: 337–67

Pullin, D. I. 1978. The large-scale structure of unsteady self-similar rolled-up vortex sheets. *J. Fluid Mech.* 88: 401–30

Pullin, D. I. 1979. Vortex ring formation at tube and orifice openings. *Phys. Fluids* 22: 401–3

Pullin, D. I. 1992. Contour Dynamics Methods. *Annu. Rev. Fluid Mech.* 24: 89–115

Pumir, A., Kerr, R. M. 1987. Numerical simulation of interacting vortex tubes. *Phys. Rev. Lett.* 58: 1636–39

Rayfield, G. W., Reif, F. 1963. Evidence for the creation and motion of quantized vortex rings in superfluid helium. *Phys. Rev. Lett.* 11: 305–8

Rayfield, G. W., Reif, F. 1964. Quantized vortex rings in superfluid Helium. *Phys. Rev. A* 136: A1194–A1208

Reynolds, O. 1876. On the resistance encountered by vortex rings, and the relation between the vortex rings and the streamlines of a disk. *Nature* 14: 477

Richards, J. M. 1965. Puff motions in unstratified surroundings. *J. Fluid Mech.* 21: 97–106

Robinson, S. K. 1991. Coherent motions in the turbulent boundary layer. *Annu. Rev. Fluid Mech.* 23: 601–39

Rodriguez, F., Mesler, R. 1988. The penetration of drop-formed vortex rings into pools of liquid. *J. Colloid Interface Sci.* 121: 121–29

Rogers, W. B. 1858. On the formation of rotating rings by air and liquids under certain conditions of discharge. *Am. J. Sci. Arts (Second Ser.)* 26: 246–58

Rom-Kedar, V., Leonard, A., Wiggins, S. 1990. An analytical study of transport, mixing and chaos in an unsteady vortical flow. *J. Fluid Mech.* 214: 347–94

Saffman, P. G. 1970. The velocity of viscous vortex rings. *Stud. Appl. Math.* 49: 371–80

Saffman, P. G. 1978. The number of waves

on unstable vortex rings. *J. Fluid Mech.* 84: 625–39
Saffman, P. G. 1979. The approach of a vortex pair to a plane surface in inviscid fluid. *J. Fluid Mech.* 92: 497–503
Saffman, P. G. 1981. Dynamics of vorticity. *J. Fluid Mech.* 106: 49–58
Sallet, D. W., Widmayer, R. S. 1974. An experimental investigation of laminar and turbulent vortex rings in air. *Z. Flugwiss.* 22: 207–15
Schatzle, P. R. 1987. *An experimental study of fusion of vortex rings.* PhD thesis, Grad. Aeronaut. Labs., Calif. Inst. Tech.
Shariff, K., Leonard, A., Zabusky, N. J., Ferziger, J. H. 1988. Acoustics and dynamics of coaxial interacting vortex rings. *Fluid Dyn. Res.* 3: 337–43
Shariff, K., Leonard, A., Ferziger, J. H. 1989. Dynamics of a class of vortex rings. *NASA TM-102257*
Sigler, J., Mesler, R. 1990. The behavior of the gas film formed upon drop impact with a liquid surface. *J. Colloid Interface Sci.* 134: 459–74
Sommerfeld, A. 1950. *Mechanics of Deformable Bodies.* New York: Academic
Southerland, K. B., Porter, J. R. III, Dahm, W. J. A., Buch, K. A. 1991. An experimental study of the molecular mixing process in an axisymmetric laminar vortex ring. *Phys. Fluids A* 3: 1385–92
Stanaway, S., Cantwell, B. J., Spalart, P. R. 1988a. A numerical study of viscous vortex rings using a spectral method. *NASA TM-101041*
Stanaway, S., Cantwell, B. J., Spalart, P. R. 1988b. Navier-Stokes simulations of axisymmetric vortex rings. *AIAA Pap. No. 88-0318*
Stanaway, S., Shariff, K., Hussain, F. 1988c. Head-on collision of viscous vortex rings. *Proc. 1988 Summer Program*, pp. 287–309. NASA Ames/Stanford Ctr. Turbulence Res., Stanford, Calif.
Sturtevant, B. 1981. Dynamics of turbulent vortex rings. *Air Force Off. Sci. Res. Rep. AFOSR-TR-81-0400.* (Available as NTIS AD-A098111)
Sturtevant, B., Kulkarny, V. 1978. Dynamics of vortices and shock-waves in nonuniform media. *Air Force Off. Sci. Res. Rep. AFOSR-TR-78-1403.* (Available as NTIS AD-A060359)
Sturtevant, B. 1979. Dynamics of vortices and shock waves in nonuniform media. *Air Force Off. Sci. Res. Rep. AFOSR-TR-79-0898.* (Available as NTIS AS-A072842)
Sullivan, J. P., Widnall, S. E., Ezekiel, S. 1973. Study of vortex rings using a laser doppler velocimeter. *AIAA J.* 11: 1384–89
Taylor, G. I. 1958. Flow induced by jets. *J. Aerosp. Sci.* 25: 464–65
Thomson, J. J., Newall, H. F. 1885. On the formation of vortex rings by drops falling into liquids, and some allied phenomena. *Proc. R. Soc. London Ser. A* 39: 417–36
Turkington, B. 1986. Vortex rings with swirl: axisymmetric solutions of the Euler equations with nonzero helicity. *SIAM J. Math. Anal.* 20: 57–73
Turner, J. S. 1957. Buoyant vortex rings. *Proc. R. Soc. London Ser. A* 239: 61–75
Turner, J. S. 1963. The flow into an expanding spherical vortex. *J. Fluid Mech.* 18: 195–208
Van Dyke, M. 1982. *An Album of Fluid Motion.* Stanford, Calif: Parabolic
Vladimirov, V. A., Tarasov, V. F. 1979. Structure of turbulence near the core of a vortex ring. *Sov. Phys. Dokl.* 24: 254–56
Walker, J. D. A., Smith, C. R., Cerra, A. W., Dogilaski, T. L. 1987. The impact of a vortex ring on a wall. *J. Fluid Mech.* 181: 99–140
Walters, J. K., Davidson, J. F. 1963. The initial motion of a gas bubble formed in an inviscid liquid. *J. Fluid Mech.* 17: 321–36
Widnall, S. E., Bliss, D. 1971. Slender body analysis of the motion and stability of a vortex filament containing an axial flow. *J. Fluid Mech.* 50: 335–53
Widnall, S. E., Bliss, D. B., Tsai, C.-Y. 1974. The instability of short waves on a vortex ring. *J. Fluid Mech.* 66: 35–47
Widnall, S. E., Sullivan, J. P. 1973. On the stability of vortex rings. *Proc. R. Soc. London Ser. A* 332: 335–53
Widnall, S. E., Tsai, C.-Y. 1977. The instability of the thin vortex ring of constant vorticity. *Philos. Trans. R. Soc. London Ser. A* 287: 273–305
Willert, C. E., Gharib, M. 1991. Digital particle image velocimetry. *Exp. Fluids* 10: 181–93
Yamada, H., Matsui, T. 1978. Preliminary study of mutual slip-through of a pair of vortices. *Phys. Fluids* 21: 292–94
Zaman, K. B. M. Q. 1985. Far-field noise of a subsonic jet under controlled excitation. *J. Fluid Mech.* 152: 83–111
Zaitsev, M. Y., Kop'ev, V. F., Munin, A. G., Potokin, A. A. 1990. Sound radiation by a turbulent vortex ring. *Sov. Phys. Dokl.* 35: 488–89

Annual Review of Fluid Mechanics
Volume 24, 1992

CONTENTS

GRÖBLI'S SOLUTION OF THE THREE-VORTEX PROBLEM, *Hassan Aref, Nicholas Rott, and Hans Thomann* 1

MODELING OF TWO-PHASE SLUG FLOW, *J. Fabre and A. Liné* 21

MEASURING THE FLOW PROPERTIES OF YIELD STRESS FLUIDS, *Q. D. Nguyen and D. V. Boger* 47

CONTOUR DYNAMICS METHODS, *D. I. Pullin* 89

PARABOLIZED/REDUCED NAVIER-STOKES COMPUTATIONAL TECHNIQUES, *Stanley G. Rubin and John C. Tannehill* 117

TOPOLOGICAL METHODS IN HYDRODYNAMICS, *V. I. Arnold and B. A. Khesin* 145

FINITE ELEMENT METHODS FOR NAVIER-STOKES EQUATIONS, *Roland Glowinski and Olivier Pironneau* 167

ATMOSPHERIC TURBULENCE, *John C. Wyngaard* 205

VORTEX RINGS, *Karim Shariff and Anthony Leonard* 235

HELICITY IN LAMINAR AND TURBULENT FLOW, *H. K. Moffatt and A. Tsinober* 281

HYDRODYNAMIC PHENOMENA IN SUSPENSIONS OF SWIMMING MICROORGANISMS, *T. J. Pedley and J. O. Kessler* 313

NUMERICAL MODELS OF MANTLE CONVECTION, *G. Schubert* 359

WAVELET TRANSFORMS AND THEIR APPLICATIONS TO TURBULENCE, *Marie Farge* 395

DYNAMO THEORY, *P. H. Roberts and A. M. Soward* 459

INDEXES

Subject Index 513

Cumulative Index of Contributing Authors, Volumes 1–24 526

Cumulative Index of Chapter Titles, Volumes 1–24 530